Int. J. Heat Mass Transfer. Vol. 22, pp. 1245–1279
Pergamon Press Ltd. 1979. Printed in Great Britain

MEASUREMENT OF DROP SIZES

B. J. AZZOPARDI
Engineering Sciences Division, AERE, Harwell, Oxfordshire, OX11 0RA, England

(*Received* 8 *November* 1977 *and in revised form* 8 *November* 1978)

Abstract—Methods for the measurement of the size of drops, solid particles and bubbles have been reviewed. A selection of methods which are potentially suitable for practical drop size measurement are presented with particular attention to their difficulty and sources of error.

It is shown that selection of a method for a specific use poses certain questions, namely:

(1) Is a mean or a distribution required?
(2) What type of mean or distribution (spatial/temporal) is sought?
(3) Is mass flux or number data also required?

The most generally applicable method is photography but this suffers from various difficulties especially for data reduction. The other suitable methods are optical and in the main do not require insertion of probes into the flow stream.

A table is included, summarising the properties of the various methods, with particular reference to the three questions posed above.

NOMENCLATURE

A, area;
A_0, area of overlap;
B, beam breadth (Figs. 16 and 18);
C, constant;
C_t, crater size, impact techniques;
d, diameter;
E, exposure, photographic;
E_{ij}, light energy, increment;
e, eccentricity;
$F(\theta)$, angular variation of scattered light;
$F(a\theta)$, tabulated scattering function;
f, focal length of lens;
$f(\ )$, probability density function;
H, probe diameter;
I, Illumination;
I_0, incident illumination;
I_c, impression coefficient, impact technique;
$i_{1,2}$, polarised scattered light intensities;
J_0, zeroth order Bessel function of the first kind;
J_1, first order Bessel function of the first kind;
K, extinction coefficient;
K_E, fraction of diameter particle permitted to move during photography;
l, probe volume length;
$N(\ )$, size distribution function;
r, distance from optical axis;
$\mathscr{S}$, signal;
T, optical path length;
t, exposure time;
t_R, residence time;
V_p, particle velocity;
V_s, scanning velocity;
W, beam width (Figs. 16 and 18);
X_c, eccentricity of intersection of circles (Appendix 1);
We, Weber number.

Greek symbols

α, dimensionless particle size;
θ, angle;
λ, wave length of light;
λ^*, fringe spacing;
ϕ, function defined by equation (18).

1. INTRODUCTION

DROPS are small discrete packets of liquid—one state in which the liquid phase can occur in two phase flows. They are very important in sprays, e.g., liquid fuel flames or spray dryers, or as entrained liquid in the gas core of annular two phase flows. Small drops are normally assumed to be spherical, the experimental evidence shows this to be justified for drops of diameter less than 3000 μm. Above this size drops are known to oscillate (e.g., Ahmadzadeh and Harker [1]).

It is more usual to find a distribution of drop sizes than monodisperse drops. The range of sizes is important in some transport mechanisms whilst in others appropriate mean values suffice. The particular mean required is usually determined by the use to which the data is to be put. In general terms means are defined as:

$$d_{pq} = \left[\frac{\int x d^p \, \mathrm{d}d}{\int x d^q \, \mathrm{d}d}\right]_{x\to\infty}^{1/(p-q)}. \quad (1)$$

The most common of these is the volume to surface area mean, d_{32}, the Sauter mean diameter, which is used in mass transfer work where the surface area governs the resistance and the volume determines the concentration. Mugele and Evans [2] and Dombrowski and Munday [3] specify other means in common use and their applications. The type of distribution can also be important particularly in the comparison of theory and experiment [4–6]. The

two main types of distributions are temporal (i.e., vary with time at one point in space) or spatial (vary in space at one point in time).

McCreath and Beer [7] point out that, for sprays from liquid fuel atomisers in furnaces, drop size frequency and spatial distribution control fundamental flame characteristics, e.g., radiant heat transfer, flame length, flame stabilisation, smoke formation, carbon carry over and formation of oxides of nitrogen. In spray drying where the drops usually consist of aqueous solutions of a chemical that is required in solid form, the drop sizes produced in the spray exert a strong influence on the product size and size distribution. These parameters are often important for subsequent processing requirements. In two phase annular or disperse flows the drop size is of great interest as it is the controlling factor in the deposition of drops onto the annular film covering the walls or the walls themselves if there is no film. This deposition is one of the mechanisms which influences the behaviour of the liquid film and hence the conditions at which the film dries out. This drying out of the film is usually termed burnout and it is most important as in constant heat flux systems (such as nuclear reactor cores) a large temperature excursion occurs when the wall film dries out. Such an occurrence is to be avoided because of the safety implications.

The results of experiments performed to date indicate that the range of sizes to be expected in the various operations are as shown in Table 1.

Table 1. Ranges of drop sizes expected

Operation	Range μm	Reference
Combustion of liquid fuels	10–800	McCreath and Beer [7]
Spray drying	10–1000	Dombrowski and Munday [3]
Annular two phase flows	10–400	Cousins and Hewitt [8]

The magnitude of the effort involved in determining a mean drop size from individual measurements is often governed by the sample size required. Large samples can sometimes be necessary to provide an accurate estimate of the population mean. Bowen and Davies [9] have estimated that, within the 95% confidence limits, the accuracy of the volume–surface mean diameter (d_{32}) for various counts varies as follows:

Table 2. Accuracy–effect of sample size

No. in sample	Accuracy %
500	±17
1400	±10
5500	±5
35000	±2

Nukiyama and Tarasawa [10] measured a minimum of 500 drops/sample and quoted an overall accuracy of ±15%.

A review of the published techniques for drop size measurement has been carried out and is presented below. Methods that have been devised for solid particles or bubbles or for drops in a liquid continuum have been examined as well as those for gas/liquid flows. Some of the methods included are obviously unsuitable for measurements within the ranges given in Table 1, but are included to illustrate an approach or to complete a picture. Both methods which provide distribution of drop sizes and those that only yield mean drop sizes will be examined, the type of result and where appropriate the type of distribution will be given in the summary table (Appendix 2). The methods will be grouped in terms of the basic phenomena employed, i.e., photographic and holographic, thermal, impact, electrical, optical, time of residence and indirect methods via velocity measurements.

2. PHOTOGRAPHIC AND HOLOGRAPHIC METHODS

2.1. *Photographic methods*

Small, swiftly moving objects are difficult to photograph. However, careful consideration of the illumination and photography involved and of the measurement of the images produced enables accurate results to be obtained with relatively simple techniques and equipment. The pertinent topics are discussed below. Methods which eliminate the photographic plate are also considered.

2.1.1. *Illumination.* The type of illumination used in any situation depends on the information sought and the geometry involved. The information sought usually has much more effect on the means of observation (of photography), the one case where it impinges strongly on the method of illumination is when velocities are sought. This is discussed at the end of the section.

Two important effects to be considered in selecting the illumination are the illumination intensity/particle size/velocity relationships and the angular variation of scattered light. The illumination required is determined by the particle size and velocity. From geometrical optics it can be seen that the light scattered from a small sphere (10–1000 μm) is

$$I = I_0 F(\theta) d^2, \tag{2}$$

where I_0 is the incident illumination, $F(\theta)$ is a function dependent on the direction of observation relative to that of illumination, and d is the particle diameter.

The exposure time is usually defined as the time

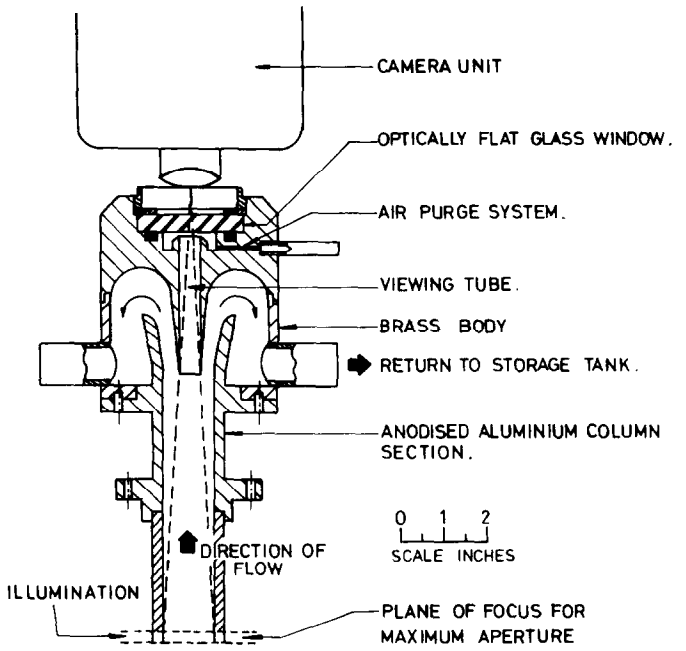

FIG. 1. Viewing system for axial photography of annular flow after Arnold and Hewitt [12].

required for the particle to move a small fraction of its own diameter so that

$$t = \frac{K_E d}{V_p}. \tag{3}$$

The exposure, the total amount of light falling on any part of the photographic plate, for the portion of the plate onto which the image of the particle has been focussed, can be expressed as

$$E = It, \tag{4}$$

and from equations (2) and (3),

$$E = (I_0 F(\theta) d^2)\left(\frac{K_E d}{V_p}\right) = \frac{K_E I_0 F(\theta) d^3}{V_p}. \tag{5}$$

A prescribed amount of light is necessary to produce sufficient activation to create a visible image on the developed plate. Therefore, if the value of E is set to this prescribed and constant value then the dependence of the incident light intensity on particle size and velocity are

$$I_0 \propto d_p^{-3}, \tag{6}$$

and

$$I_0 \propto V_p, \tag{7}$$

i.e., the smaller and faster the particle the more illumination required.

The theories of Fraunhofer diffraction and Mie scattering have shown that $F(\theta)$ increases as θ, the angle included between the illuminating and observing light paths, tends to 0°. Therefore the illumination is governed by particle velocity and size and the illumination should be as close to 0° to the observing direction as possible (if it is 0° then shadows of the objects will be recorded).

The geometries involved can be divided into two main groups. The first consists of sprays which are in the open or in containers with adequate observation facility. These can be photographed perpendicularly to the direction of main flow using back or side illumination.† When the drops are flowing in a container (e.g. tube) with walls that are not transparent, e.g. if the tube walls are covered by a wavy liquid film as in annular two phase flows, then the flow must be modified by stripping off the film and observing/illuminating as for the first group or axial photography must be used (Fig. 1 and [12]). When the film has been removed the resulting jet containing the spray may be observed in free air [13, 14]. This confines the method to atmospheric pressure experiments.

When back illumination is employed the drop is seen as a black dot (or dash if moving) on a bright background. The dash or elongated dot would occur if the drop has travelled an appreciable distance during the exposure. Kirkman and Ryley [15] have determined that the width of the dash is only directly proportional to the drop diameter if the exposure time is short enough to limit the travel of the drop to two diameters. Otherwise a reduced image is recorded by the photographic emulsion. When drops are illuminated from the side they appear as bright

†When drops burning in spray are to be photographed special precautions are necessary otherwise the luminosity of the flame will overwhelm the photographs. McCreath *et al.* [11] give recommendations regarding the most suitable wavelength of illumination and the filters and photographic film most suited to minimise the effect of the flame luminosity on the photographic film.

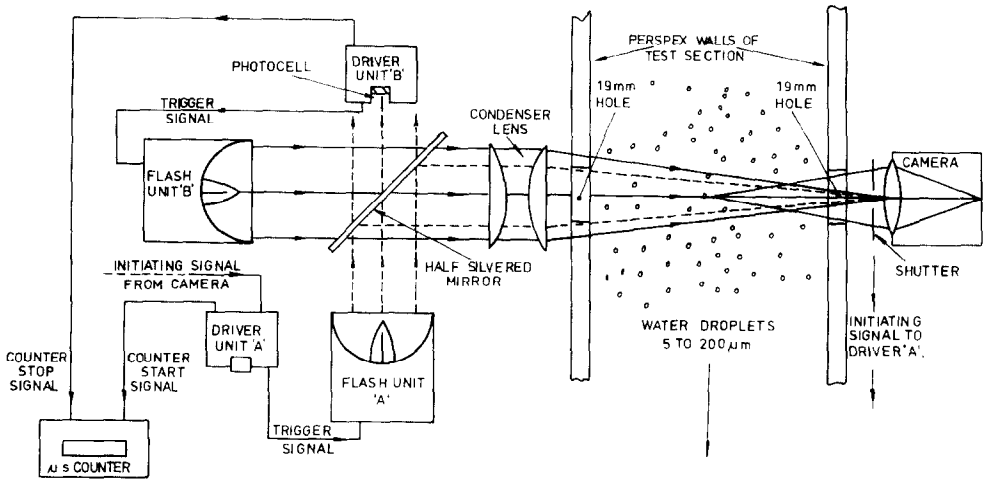

FIG. 2. Double flash technique of Finlay and Welsh [17].

dots on a dark background. If semi-automatic methods of data abstraction are to be used then illumination of the field of interest from both sides is recommended because with one-sided illumination the drops may not appear as complete circles. This would make it difficult to set up some of the data abstraction systems. For axial photography side illumination is, of course, necessary and again two synchronised sources are recommended. A more thorough method of supplying uniform illumination is to use an elliptical mirror as used by Treleaven and Tobgy [16] in their photochromic dye irradiation experiments. A light source placed at one focus of the mirror will irradiate any object, e.g. the test section, at the other focus uniformly.

If the direction of motion and velocity of the drops are also sought a double exposure technique must be used. Use of a single streak length is not recommended as the method is not accurate; flash sources tend to have fast rise times and slow decay times, therefore one end of the streak is usually blurred. It is, consequently, considered good practice to use double flash exposures and to take measurements from the start of one streak to the start of the next. Multiple flashes are most conveniently provided by a stroboscopic light source. However these units do not always provide sufficient intensity of illumination and/or a fast enough rate of interruption. Therefore special units have been produced. McCreath *et al.* [11] describe a double flash unit where the first spark is focussed at the point of origin of the second spark by a lens system, a further lens focusses them both onto the camera shutter thus illuminating a small area of the spray. The spark sources can be fired consecutively at electronically controlled times and the delay time between them may be monitored by a suitably placed photocell. This technique has been designed for back illumination. A similar technique has been described by Finlay and Welsh [17]. In this case two flash units are arranged so that their directions of illumination are at right angles to each other and one of the units faces the object. A half-silvered mirror is placed at the intersection of the light paths and at 45° to each (Fig. 2). Electronic circuitry is provided to trigger the units sequentially and to measure the delay time involved.

2.1.2. *Observation.* The small size of the drops to be photographed makes a large magnification necessary. Whether this is applied directly or in two stages depends on several factors—the fineness of the grain of the photographic emulsion employed, the size of field to be photographed and the method of abstraction. Williams and Hedley [18] report magnifications used as being no greater than $\times 30$ and total projected magnifications of the order of $\times 100$. This gave a lower limit of discernible particles of 5 μm. However a large magnification at the photographic stage usually requires small image distances which in hostile environments such as flames is not easily realised. Large magnifications are usually produced in conjunction with small depths of field. Therefore particles outside small elements on either side of the plane of focus are not clear and, in the extreme not visible. The limits of the depth of field are usually defined with respect to a circle of confusion, i.e. the smallest diffuse image of a point that is indistinguishable from a point.† Several formulae exist which relate depth of field to the other relevant parameters, such as magnification, aperture (f No.) and focal length of lens; for example Cox [19] gives

$$d = \frac{2fN(M+1)}{100M^2}. \tag{8}$$

where f is the focal length of the lens, N is the aperture, and M is the magnification.

The difference in object distance between objects at the near and far boundaries of the field in focus are usually small so there will at most be a minute error in the magnification scaling that should be

†Dombrowski and Weston [20] use the definition of the distance over which diameter can be measured to within $\pm 2\frac{1}{2}\%$ of its real size.

applied to the photographs. However a small depth of field is not always compatible with the requirements of a particular situation as for example when spatial distributions are fairly important. In these cases where large depths of field are necessary the magnification error due to the different object lengths can be significant. Several methods can be used to overcome this problem of a large possible range of positions and hence magnifications when the depth of field is large, e.g. stereoscopy and simultaneous observation of several neighbouring planes each of small depth of field can both provide exact image distances.

by Whalley *et al.* [23] in which annular two phase flow was photographed in a manner similar to the axial method mentioned above. A lens/prism system created a pair of stereo-images per frame. The viewing axis was not coincident with the tube axis as the equipment was designed to examine waves on the film flowing along the tube wall. An examination of several photographs taken in this way has shown the difficulty in matching pairs of images of a drop, e.g. Fig. 4, and so no drop size data has been abstracted from this work.

A technique for enlarging the depth of field has been proposed by Dombrowski and Weston [20].

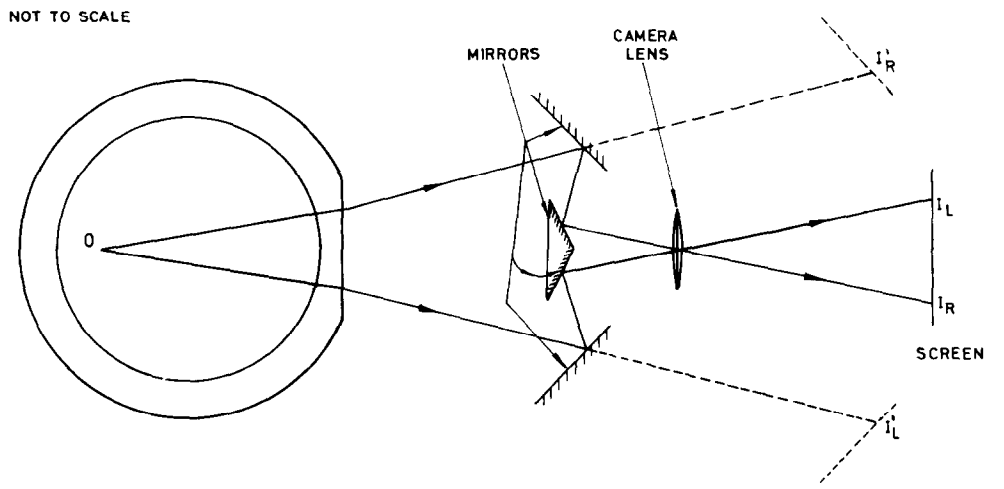

FIG. 3. Mirror stereo-attachment after Reddy *et al.* [22].

The stereoscopic technique was used by Wakstien [21] and Reddy *et al.* [22] to measure velocities in pneumatic conveying. Stereoscopy provided the position of the particles, stroboscopic illumination was used and the velocities were obtained from the distance between interruptions on streaks and the time interval. The method can be applied to the measurement of particle size, whether on its own or in conjunction with velocity measurements. The version used by Reddy *et al.* [22] is shown in Fig. 3; they used mirrors to focus two views of the field of interest onto one frame. The views were observed from different directions so that the relative positions of the images of an object were related to the position of the object and from the former the latter could be obtained and hence the magnification deduced. The full relationships required for the determination of the position of the object and the magnification are very complex but can often be simplified with little loss of accuracy, they can also be checked by calibration. The difficulties involved in stereoscopy are not specific to its use in drop size measurements but apply generally to stereoscopic methods for velocity and position determination. The main difficulty is the identification of the pairs of images of an object which can be very tedious. A variation of the method was used

The technique was designed to follow particles that moved in and out of focus and so could be used to examine a larger volume than is normally possible while minimising magnification error. The technique is best explained by reference to a simple ray diagram for the formation of an image, Fig. 5. An object at plane A is in focus at the plane of the photographic plate. If the object moves to position B it moves out of the depth of field about A and hence out of focus. Therefore to ensure that the planes corresponding to the two positions of the object are in focus simultaneously a second photographic plate must be placed at the image plane of B. To accomplish this two cameras could be aligned on the object by means of a beam splitter with one focussed on plane A and the other on plane B. Selection of planes whose depth of field just overlap gives a continuous volume of observation. A more convenient arrangement is to insert a beam splitter on the image side of a single lens and to place the photographic plates in appropriate positions as shown in Fig. 6. Obviously more beam splitters could be used further enlarging the volume of interest, the main limitation to the number of beam splitters would be imposed by the intensity of illumination available as at each beam splitter a division of the light is effected.

FIG. 4. Stereo and semi-axial photography of annular two phase flow (Whalley *et al.* [23]).

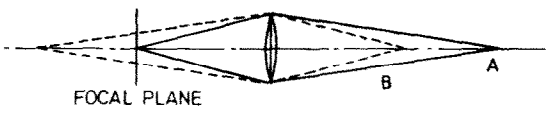

FIG. 5. Problem of large field of view.

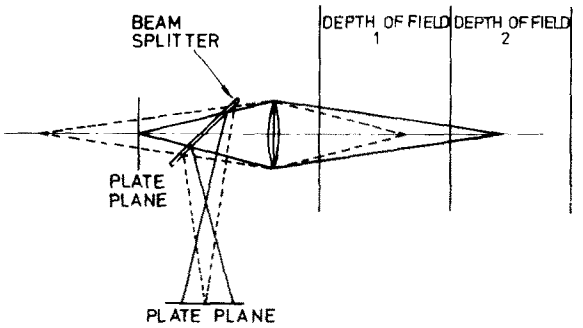

FIG. 6. Solution to problem of large fields of view, Dombrowski and Weston [20].

An alternative technique for examining large volumes while still defining object positions closely would be to use light of different colours. If several narrow neighbouring planes are illuminated each by light of a different colour and the whole volume photographed using colour film, under conditions that give a large depth of field, then the colour of the particles should indicate their positions and hence the magnification involved.

It is common practice to identify particles in focus by making a subjective judgement regarding the sharpness of the images involved. De Corso [24] has used a more objective approach. Fresnel fringes, alternate rings of light and dark, are formed around a drop when it is back-illuminated. The width of the first fringe is a linear function of the displacement of a drop from the plane of best focus for both positive and negative displacements.† Therefore by examining drops with fringe widths less than preset values only drops that are "in focus" are considered, i.e. drops within close limits on either side of the plane of best focus. De Corso claims errors of 10% for 5–10 μm drops and 0.5% for 500 μm when he limits examination to particles within ±640 μm of the plane of best focus (camera magnification ×10, overall magnification ×100).

Another approach which could help identify infocus drops has been suggested by Birch [25]. His approach involves spatial filtering to remove the zero spatial frequency. The consequence of this is that

†Positive displacement is between the plane of best focus and camera.

diffracting object structure is imaged with enhanced contrast because object areas of constant or slowly varying transmission are suppressed. The edge of an infocus drop has a rapid change of transmission and is therefore seen very sharply whereas the transmission round an out of focus drop varies slowly and is thus suppressed. Practically the filtering is affected by using an illuminating system which produces a plane coherent wavefront and an imaging system in which the spatial frequency content of the image may be modified by the introduction of a filter in the anterior focal plane of the projector lens. The filter usually takes the form of a grating.

2.1.3. *Abstraction of data.* Visual sizing and counting methods are very tedious and suffer from a bias imposed by the operator who usually has to use subjective judgement in placing individual particles into a size group. It has long been known that this bias (or error) could be large. This is illustrated by the following examples:

(1) Nukiyama and Tarasawa [10] claimed a personal error in counting of 7%;

(2) Biggs and McMillan [26] found an inter-observer coefficient of variation of 3.1% and a random error in the count of 7.8% when samples of 450 were examined;

(3) Heywood [27] found a range of 15.5% in the estimates of mean size by 10 observers when opaque circles (placed adjacent to the items being sized) were used and 4.6% when transparent circles (placed over item) were used. The overall mean estimate of size was 5.7% high with the opaque circles and 1.9% high with the transparent ones;

(4) Watson and Mulford [28] found biases ranging from −17% to +13% amongst 9 observers.

These examples are all specific to microscopic counting and sizing however similar problems should be guarded against when measurements are taken from photographs. Therefore aids to visual counting and sizing such as the transparent circles mentioned by Haywood [27] are necessary. Non-visual techniques are obviously preferable.

McCreath *et al.* [11] describe a semi-automatic apparatus which punches the coordinates of a point onto paper tape when a set of cross hairs are set over the point and a button is pressed. From the coordinates of two diametrically opposed points on a particle the diameter is obtained. Similar units are available commercially (e.g. "OSCAR" by Benson-Lehner and "DMAC" by CTEX).

Some of these units can be interfaced directly to a mini-computer and hence output format is at the discretion of the programmer. The accuracy of these units can be very high particularly those where the scaling can be preset by the operator, any error will be masked by operator error.

Morgan and Meyer [29] and Ramshaw [30] both describe automatic data abstracting apparatus capable of detecting and sizing images of particles and of discriminating between those in focus and those not. Both units described work on the same principle, as microdensitometers. In such instruments a spot of light is traversed across the negative and the portion of light transmitted is measured. When the particle image, an area of one density on a contrasting background, coincides with the spot then a change is observed in the output of the light detector. The instruments can usually differentiate between images that are in focus and those that are not as the sharp edges of the former yield a step-change in output whereas the latter with their blurred edges give a ramp change. However, for this distinction to be possible the diameter of the scanning light spot must be very small as the response to a step change in density is a ramp change in output with width twice the spot size (microdensitometer averaging error). Thus the microdensitometer averaging error could be confused with the blurring at the edges of an out of focus particle. It is preferable that the images observed be larger than the scanning spot, otherwise problems will arise regarding coincidence (the presence of more than one particle image within the light spot). If the spot is smaller than the image the size is obtained from the traverse time and the scanning velocity. This, of course, measures a chord, not necessarily a diameter, so that a transformation of the data in a manner similar to that of Herringe and Davis [31] is required.

A variation of this technique is used by the Quantimet series of instruments. In this case the density is determined at a series of points on a rectangular grid. The number of points that display a different density is then counted, this represents the projected area of a particle if there is only one within the area of observation. The instrument contains sorting logic to group the data into preset size ranges. It can examine material in any of several forms, e.g. photographic prints, projected negatives etc. For an example of its use in drop sizing see Yule *et al.* [32].

2.1.4. *Photography related methods.* Techniques which eliminate the photographic plate have recently been presented by Simmons [33] and Dix *et al.* [34]. They have both replaced the photographic plate by photodetector arrays. Simmons has used a simple inline system with a purge system to keep the lens clear of drops and with the photodetector array at the focal plane of the camera. He moves the spray nozzle under consideration so as to examine different parts of the spray whilst keeping his illumination and observation modules stationary. The photodetector signals are sorted by a computer. Dix *et al.* [34] use a straight through system using parallel light and no lens (shadowography). They also use a focusing system (Fig. 7). By distinguishing between drops in focus, nearly focused and completely out of focus they can obtain information regarding the longitudinal positions of drops. The outputs of the two detector arrays are electronically formatted and punched onto tape for subsequent analysis on a computer. This technique is therefore capable of giving x, y, z, t data.

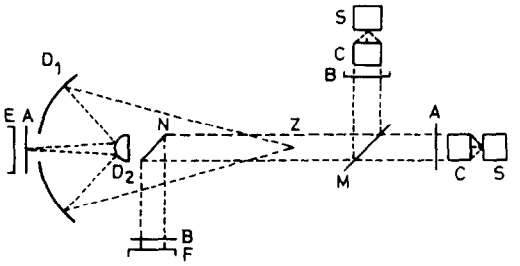

FIG. 7. Optical system (Dix *et al.* [34]).

2.2. *Holographic methods*

Photographs are a two dimensional representation of three dimensional scenes. In contrast, holograms, the interference pattern formed by light scattered by the object and light unaffected by the object, "freezes" three dimensional scenes which can be recreated in their entirety at leisure. Figure 8 indicates the requirements for the formation of a hologram. A beam of coherent light, after being split in two, illuminates the object. The light reflected by the object onto the photographic plate on which the hologram is to be formed arrives at the same instant as a reference beam that has been deflected round the object unchanged in phase. The phase difference between the two beams causes interference to take place and the recorded hologram is composed of regions of high and low light intensity. Examination of the hologram requires reconstruction which is affected by illuminating the hologram with the reference beam from the same direction as during the recording. The hologram acts as a diffraction screen for the reference beam and a wave pattern is formed, behind the hologram, which to an observer looks just like the original object.

The original work on holograms [35] used Fresnel (or near field) holograms but later work has concentrated on Fraunhofer (or far field) holography because it eliminates the troublesome virtual image that appears as an out of focus image in place of the real image in Fresnel holograms.

The advantages of holography are:

(i) Little restriction on the depth of field; and

(ii) Uniform magnification for drops separated longitudinally when a reconstructed hologram is projected.

The depth of field has been empirically assessed to be $100d^2/\lambda$, where d is the drop diameter and λ the wavelength of the illumination employed.

Reconstructed holograms have been examined by taking photographs of the hologram. These could then be used conveniently. Alternatively the hologram could be examined directly by one of the facilities of the Quantimet instrument (Section 2.1.3). To ensure that particles are seen as stationary objects it is recommended that movement during the production of the hologram be restricted to 10% of the fringe spacing. Pulsed ruby lasers produce an exposure of about 30 ns, which essentially renders motionless particles moving with velocities up to 100 ms^{-1}. However, for these pulsed lasers with their short coherent lengths it is recommended that the inline system used by Gabor [35] be employed in order to make the angle between the object and reference beams as small as possible.

Attempts have been made to use holograms to size submicron particles, however the conclusion reached

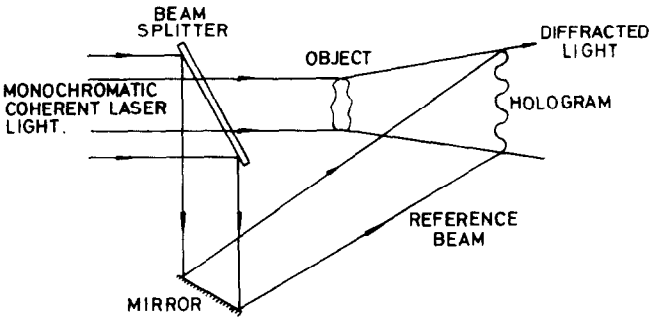

FIG. 8. Holography schematic for production of holograms.

[36] was that though these particles, which can be considered as point scatterers, can be located their size cannot be determined from the holograms. Thompson [37] considers the minimum size which can be measured by holography to be 2 μm.† Upper limits in the millimeter range have been quoted by some workers. The holographic technique has been used to measure particle size by Fourney *et al.* [38] and Webster [39]. A commercial system is offered by N.E.L.

3. IMPACT METHODS

3.1. *Sampling slides*

Drops may be sized by microscopic examination after capture on solid surfaces or in thin, viscous liquid films. Capture can be effected by either exposing the solid substrate on which the solid or liquid film is spread, to the flow to be sampled or by drawing a stream of the drop laden fluid past this substrate. The latter method suffers from all the obvious disadvantages of interfering with a two phase system while interest centres on the flow

†Extra magnification could be obtained by using light of different wavelengths for taking and viewing the hologram [37a].

structure and not only on the composition. In any technique where the sample is taken off precautions have to be taken to ensure that a representative sample is collected and analysed. The best approach is that of isokinetic sampling, i.e. ensuring that the velocity in the probe is equal to that outside. These velocities are usually equalised by adjusting the take off rate until the static pressures inside and outside the probe are equal. Failure to equalise the velocities results in a surfeit of larger particles if the take off rate is too low, and a deficit for too high a take off rate. Allen [40] presents correction factors for anisokinetic sampling.

In addition the work of Ranade *et al.* [41] shows that for particles within the size range shown in Table 1 deposition of drops onto the sample tube walls occurs even when a secondary gas stream is injected through the porous walls of the sample tube.

The former method required a fast moving mechanism if the sampling device is not to be swamped by drops. Such a fast moving mechanism could set up a perturbation in the flow and distort the flow structure. Various workers have either traversed the sampling device rapidly across the flow stream or exposed it briefly to the flow by opening normally closed shutters. In spite of these difficulties the method has been widely used.

The solid-coated substrate often consists of a glass microscope slide, for as May [42] has noted "there is no doubt that the $3'' \times 1''$ microscope slide is superior to all other forms of materials on which to deposit material in respect of ease of handling, examination, cleaning and availability." These slides could be coated with a solid thin film such as Magnesium oxide, soot or vaseline or with a liquid of which the recommended ones are mineral oil/vaseline or silicone oil/silicone grease [43]. In the case of solid coatings the impacting drop produces a crater whose size is drop size dependent. Several relationships have been proposed for drop size in terms of crater size, they are usually of the form:

$$d = I_c C_t, \tag{9}$$

where d is the drop diameter, I_c is an impression coefficient, and C_t is the crater size (diameter).

May [44] has determined I_c to be 0.86 for drops in the range 20 to 200 μm and 0.71 for 10 μm drops. Stoker [45] has used the empirically determined relationship,

$$I_c = 0.77 We^{0.2}, \tag{10}$$

where We is the Weber number for the drop.

With liquid coatings the drop is captured whole and thus can be measured directly.† In some cases the drop is distorted to a lens (i.e., flattened because its diameter is greater than the film thickness) and a correction factor, the flattening coefficient must be applied. Putnam *et al.* [46] have given methods for the determination of this coefficient.

A problem encountered in these sampling techniques is the shattering of drops on impact. A method of controlling the speed of impaction is therefore required. Hence the resort to external sampling. Another problem is by-passing of the sample slide. Small drops tend to follow the continuous phase about the slides and hence not deposit in contrast to large drops whose inertia causes impact. Narrow slides enable smaller drops to be captured but in the limit one would require a slide width of the order of the drop size.

3.2. *Cascade samplers*

Use is made of the by-passing problem discussed above in cascade samplers (or impactors). These are devices containing a series of carefully designed nozzles and baffles. Drops of different sizes are directed into chambers where they are either allowed to coalesce or they are caught on coated slides as in the last section. In the coalescence method the collected volume in each chamber is measured and the number of drops estimated. All drops in a chamber are assumed to have the mean diameter for which the chamber was designed.

The impaction slides are examined microscopically and equation (9) is applied. May [42] has reviewed nozzle design and suggested slot jets to be the best as they minimise end effects and produce a ribbon deposit which is very useful in the microscopic examination. Ellis *et al.* [47] have produced a 2 stage cascade designed for liquid drops in an atmosphere of their own vapour (prevention of condensation/evaporation).

4. THERMAL METHODS

4.1. *Evaporation methods*

The evaporation of a drop in the Leidenfrost mode, i.e., hovering on a cushion of vapour produced from its surface, on a hot surface can yield an evaporation time that is drop size dependent [48]. The method consists of impinging the drop onto a hot surface and then observing its evaporation. An alternative technique, which does not suffer from the problem of having to impinge the drops onto a surface, uses a thin hot wire [49, 50]. When operated in a drop-laden atmosphere, heat is removed from the hot wire through forced convection by the vapour or through evaporation of drops that impinge on the wire.† Whenever a drop impinges on the wire it causes a large spike to occur in the heat dissipation, the area under this curve (base line, normal vapour convection heat removal) is proportional to the drop volume. Problems arise in that the wire has to be strong enough to withstand drop impact and that some smaller drops would tend to by-pass the wire, i.e., they would follow the gas flow

†Note must be taken of the fact that refractive effects would distort the appearance of the drop and therefore appropriate correction should be made.

†It is much easier to impinge drops onto a thin wire than onto a flat surface—see comments in Section 3.1.

as in the impaction method above. The method would yield a temporal distribution if a hot wire were used, the distribution produced by the hot surface method would depend on the dimensions of the surface.

4.2. *Freezing methods*

An alternative thermal technique is to freeze the drops and then analyse them by means of standard solid particle sizing methods, such as sieving, whilst keeping the temperature sufficiently low to maintain solid drops. Alcohol in a dry ice bath [51] and liquid nitrogen [52] are the more popular freezing media. This method is obviously not suitable for liquids in equilibrium with their own vapour. Long distances can be necessary to freeze drops during flow which is a disadvantage. Also care must be taken (when air is the vapour phase) that no carbon dioxide be present. Otherwise a freezing temperature between those of water and carbon dioxide must be used to prevent liquefaction or solidification of the carbon dioxide.

A variation of this method specific to kerosene modelling in isothermal experiments is the use of a suitable wax at temperatures just above its melting point. Such a wax has similar physical properties to kerosene. These working temperatures tend to be just above room temperature and close to the melting point so that the drops are quickly frozen.

5. ELECTRICAL METHODS

5.1. *Resistive/capacitive*

The methods described here use either the low resistivity of the drop to complete a bridge between a pair of needle electrodes or the difference in electrical properties of the phases to employ the resistance/capacitance between a point electrode and the conducting tube wall. The methods using the latter technique were designed for bubbly or solid/liquid systems and so are not directly suitable for drop systems but the equivalent technique using capacitance might be applicable.

The needle bridging method developed by Wicks and Dukler [53] has been further examined by McVean and Wallis [54], Pye [55], Jones [56] and Jones and Sargent [57]. Two needles, in line with each other with their tips a short distance apart, are connected in a circuit with a resistance and a battery. When a drop completes the bridge an electrical pulse goes through the resistance and is monitored. To make the pulse more visible to counters it has been found helpful to pass the pulse through a circuit whose output is a square wave. A pulse signifies that a drop larger than the needle spacing has bridged the gap. The experiment is started with the gap set at a large distance, the setting is then reduced progressively and mean count rates obtained for each setting. This provides a set of data which could be reduced to the drop size distribution. Wicks and Dukler presented a reduction procedure but McVean and Wallis have pointed out an error in the method, conceded by the original authors, which if corrected would have invalidated the reduction scheme. This is because the recursive technique employed to solve for the drop size distribution function cannot be used as it produces error magnification. The basic problem appears to be that the kernel of the integral expression of Wicks and Dukler is weighted towards large drops. McVean and Wallis have produced a simple method for determining the cumulative volume distribution from the count data obtained. In cases where the count frequency is less than 2 kHz the probability of the simultaneous presence of two drops, with its consequent problems, is expected to be small as the pulse rise time is only 10 μs. From cine films made by Pye it is seen that drops break away cleanly. However Jones and Sargeant [57] have carried out careful experiments on this double needle technique. They found the technique was difficult to use because the apparent resistance of the water/glycerol drops, used as models for fuel oils, bridging a pair of needles is:

(i) Large ($> 10^9$ ohms);
(ii) Dependent on the velocity of the drop;
(iii) Dependent on the surface conditions of the needles;
(iv) Dependent on the immersion of the needles into the drop.

Also the electronic processor needs to be very fast acting so as to be able to respond to the very rapid changes in resistance. As this is not easy to satisfy, problems arise in the counting procedure. Jones and Sargeant conclude that the Wicks–Dukler technique could be satisfactory, from an experimental aspect, for drop size measurement where the drops are large and slow moving. They were not able to specify the range of applicability any more specifically as the results will depend on the equipment used in any given application.

The first of the phase property difference methods was developed by Beck *et al.* [58]. They showed that analysis of the autocorrelation function of a signal obtained from an alternating current conductivity transducer (current measured between a point electrode at the tube axis and the tube wall) gave a measure of the particle size of a flowing sand/water mixture.† Because large particles follow large eddies and small particles small eddies the mean particle size could be measured by allowing the normalized signal from a correlator to be split in two. The resulting signals were passed through high and low pass band filters respectively resulting in unequal signals because of the different frequency spectra of large and small eddies. The ratio of the signals can be used, after calibration, to measure the mean particle size. For drop/gas flows the equivalent technique using capacitance instead of conductance must be considered. (See Beck *et al.* [59] who report such an approach for mass flux metering.) The method is, of course, confined to flow in tubes.

†The method was originally devised to measure mass fluxes.

5.2. *Charge removal methods*

If a length of wire or other small metal object is held by an insulated connector/support in a drop laden steam and charged to a high potential, then, when a drop impinges on this detector, it will take up some of the charge. The charge lost may be monitored and if there is a relationship between charge and drop size then the method can be used to monitor individual drop sizes. Giest *et al.* [60], Gardener [61], Guyton [62], Steen and Chatterjee [63] and Tatterson [64] have determined that charge/dropsize relationships do exist. However the exact form appears to be in dispute as Guyton [62] and Steen and Chatterjee [63] found the pulse to vary as the square of the drop diameter, whilst Giest *et al.* [60] found it to vary as the drop diameter to the 1.6 power. This functional dependence has not yet been explained fully. Steen and Chatterjee [63] try to explain the dependence by examining the two asymptotic cases of small probe/large drop and large probe/small drop. For the small probe and large drop they argue that the capacitance approaches that of a sphere and a point charge and therefore the capacitance varies with d. However for large probes and small drops, when they are of similar size, they can be equated to parallel plates so that the variation should be as d^2.

Tatterson [64] used two probes, a wire stretched across the prongs of a fork shaped support and a metal sphere at the end of a support arm. He calibrated them by means of streams of uniform drops produced at a vibrated nozzle and found a d^2 relationship.

If the probe is constructed from wire the field will not be uniform over it and charge removal will vary not only according to the drop size but also as to the position of drop impingement. Drops striking the wire near its tip are charged to a higher potential than those striking elsewhere on the probe because of accumulation of charge near the tip. Gardener [61] has suggested masking the tip to overcome this problem. The shapes of Tatterson's probes were, no doubt, selected to comply with this suggestion but care must be taken that variations in potential do not exist in these cases. If drops are not removed from the probe they could build up, form a continuous film and short out the equipment.

The output of this technique would be a series of discrete drop sizes which must be sorted and counted.

6. OPTICAL METHODS

6.1. *Scattering methods*

6.1.1. *Background.* The intensity of light scattered by a particle depends on the intensity of the illuminating radiation, the diameter and refractive index of the particles, the wavelength and polarisation of the light and the direction of observation relative to that of illumination. The theory of scattering was formalised many years ago by Mie [65] who, on the basis of electromagnetic theory, obtained a rigorous solution of the diffraction of a plane monochromatic wave by a sphere of any diameter and of any composition situated in a homogeneous medium. For details of this theory the reader is referred to the excellent books by Kerker [66] and van de Hulst [67]. Calculations based on this theory have showed that the scattering by a sphere varies in a complicated oscillatory fashion with angle of observation, and that the particular pattern depends on both the size parameter, $\alpha = \pi d/\lambda$, and the relative refractive index. These calculations have been confirmed by experimental measurements, for example, Blau *et al.* [68] have found good agreement between calculations using Mie theory and experimental measurements from single particles in suspension held in place by an electrostatic field. They examined particles up to 100 μm. For particles larger or smaller than the wave length of light, simpler theoretical approaches have been produced. In the latter case the theory of Rayleigh applies, the former can be approached through geometric optics. This angular distribution of scattered intensity can be used for sizing particles as can variations in colour or polarisation. However, their use tends to be confined to particles smaller than the range considered here, i.e., < 1 μm (Kerker [66] gives examples of the different approaches). For larger particles, $d \geqslant 10$ μm, the intensity of the light scattered at a given angle is directly proportional to the square of the diameter. However, as drift and fluctuation of the monitoring equipment could interfere with the measurements, the use of absolute measurements of intensity are not recommended. The above has referred to single spheres. If more than one sphere is present it is usually assumed that the scattering by an array of particles is incoherent so that the scattering functions corresponding to an isolated particle may be used. The cumulative effect is obtained by adding the intensity scattered by each particle. It is also assumed that there is no multiple scatter (rescattering of scattered light). These assumptions are usually fulfilled when particles are randomly positioned in space and a sufficiently dilute system is considered. The total amount of scattered light only deviates from the square law dependence at very small particle sizes as can be seen from a plot of the scattering coefficient, K (Fig. 9). The behaviour below 1 μm is monotonically increasing but between 1 and 10 μm the K/d relationship oscillates, above 10 μm K is independent of diameter. Therefore an approach via total light scattered is only feasible for drops smaller than 1 μm. K is defined as:

$$K = \frac{1}{\pi} \int_0^{\pi} \int_0^{2\pi} I_{sca}(\theta, \phi) \sin\theta \, d\theta \, d\phi. \qquad (11)$$

However, the ϕ relationship is of a simple form. Therefore this part can be integrated over 0–2π and the expression reduces to:

$$K = \frac{1}{\alpha^2} \int_0^{\pi} (i_1 + i_2) \sin\theta \, d\theta, \qquad (12)$$

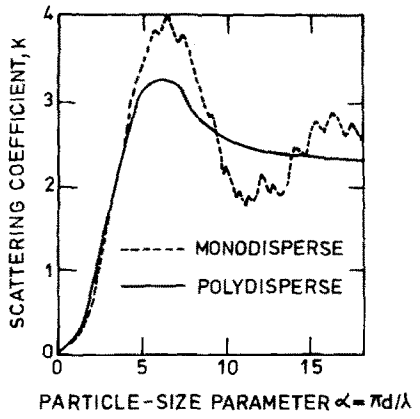

FIG. 9. Scattering coefficient.

(Kerker pp. 49 and 392) where i_1, i_2 are the intensities of the scattered light of perpendicular and parallel polarisation, θ is the angle between the irradiation and observation directions, and α is the nondimensional particle size ($\alpha = \pi d/\lambda$). i_1 and i_2 are dependent on particle diameter, wavelength of light and relative refractive index of the particles. The effect of the simultaneous presence of several sizes can be seen from Fig. 9 only to be felt below $\sim 1\,\mu$m.

For scatter at very small forward angles the particle tends to behave as an opaque disk and diffraction occurs about it. The angular distribution can be described by the Airy pattern, which is normalised to give unit intensity at zero deviation and is described by:

$$I\alpha\left[\frac{2J_1(\alpha\sin\theta)}{\alpha\sin\theta}\right]^2 \tfrac{1}{2}(1+\cos^2\theta), \qquad (13)$$

which for small angles reduces to:

$$I\alpha\left[\frac{2J_1(\alpha\theta)}{(\alpha\theta)}\right]^2, \qquad (14)$$

where J_1 is a Bessel function of the first kind and α, θ have been defined for equation (12). This function, shown in Fig. 10, is the main component of small angle forward scattering (the minor components being refraction and reflection). The function has zeros that are size dependent and can thus be used for sizing. The cumulative intensity for solid angles

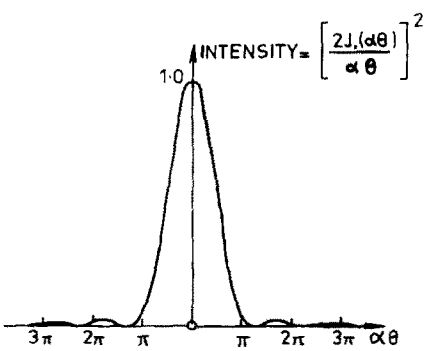

FIG. 10. Airy function—distribution of light diffracted by an opaque disc.

increasing from zero can be written

$$E' = Cd^2[1 - J_0^2(\alpha\theta) - J_1^2(\alpha\theta)], \qquad (15)$$

where E' is the light energy diffracted within the solid angle $\pm\theta$, and J_0, and J_1 are Bessel functions of the first kind (zeroth and first order respectively).

6.1.2. *Scattering from single particles.* In spite of the problems described above regarding the use of absolute measurements of intensity, methods have been developed which examine the scatter from a single particle at a fixed angle. These methods suffer from the problems of coincidence (the presence of two or more particles within the probe volume) and edge effects (illumination or observation of only part of a particle). Use of a narrow parallel beam of illumination and of a similar observation beam allows a small probe volume to be defined thus minimising the chance of a coincidence. The inclusion of a discriminator in the electronic circuitry would enable one to reject the signal arising from the coincidence of two particles as such a coincidence will produce a doublet pulse. The probability of a coincidence occurring in such a way so as not to produce a doublet is very small indeed. The problem of edge effects—when a particle is only partially in the probe volume—can be guarded against by surrounding the cylindrical light beam by an annular beam of light of a different colour. By means of beam splitters and filters the signal from each colour could be monitored separately. Then, the use of appropriate circuitry would enable particles only partially in the probe volume to be identified as they would give a simultaneous signal in each colour.

Most of the workers who have used this method examined the scattering at single angles in the range 30 and 60°. Landa and Tebay [69] and Keller [70] have examined bubble sizes by this method, and Mason and Ramanadham [71] have produced such an instrument to examine rain drops. Shofner *et al.* [72] have also produced a single particle scatter instrument (available commercially) using a pulsed light source. None of the workers mentioned above allowed for the problems of coincidence or edge effects. This type of approach obviously provides data on individual particles which must be collected and sorted.

6.1.3. *Multiple particle scatter.* The scatter from several particles of the same size, given sufficient separation, can be summed. However to determine the particle size from this summing the concentration must be known. The scatter from mixtures of different sized particles can also be summed weighted with the fraction of each size present. For particles of the range shown in Table 1 the forward direction is the only region where the intensity variation is sufficiently sensitive to provide particle size information; the sensitivity arises from the dominance of diffraction effects in forward scatter. For smaller particles ($< 10\,\mu$m) the light scattered over the whole range of angles (0–π) can be used, e.g. Carabine and Moore [73].

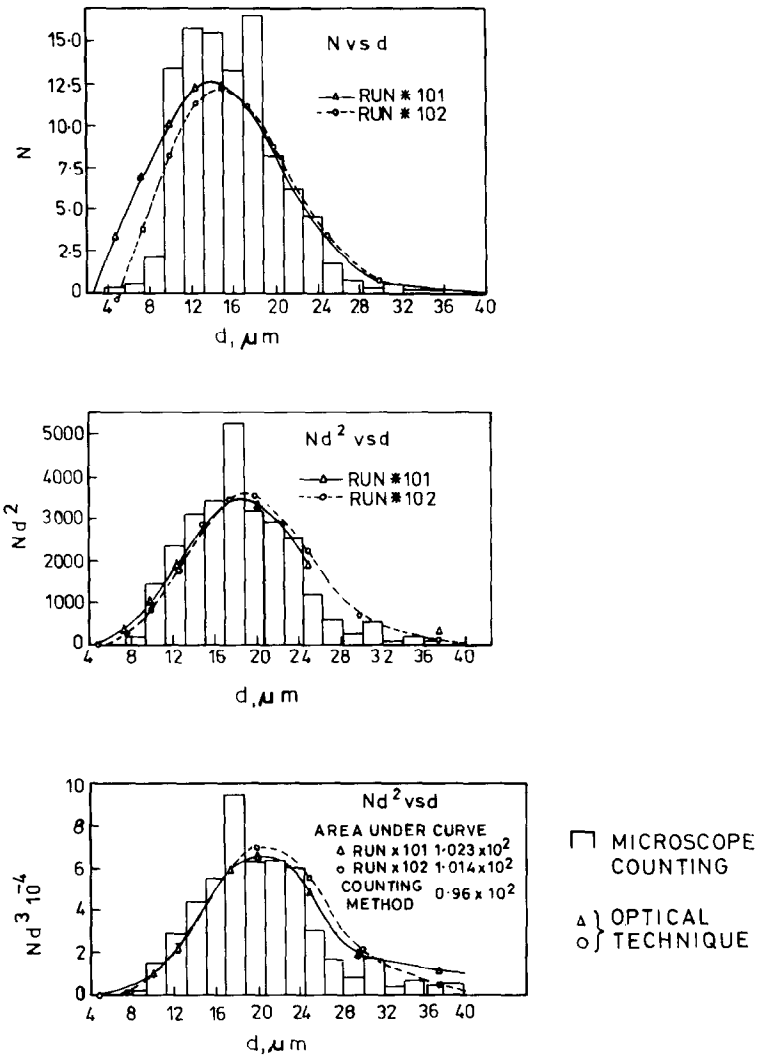

FIG. 11. Results of Chin *et al.* [77].

Dobbins *et al.* [74] examined the small angle forward scatter for a polydispersion described by an upper limit log normal distribution. They found the scattered light distribution to be insensitive to variations in the parameters that described the particle size distribution. This led Dobbins *et al.* to confine the method to yield the Sauter mean diameter. In contrast, Deich *et al.* [75, 76] and Chin *et al.* [77] considered the size/light distribution relationship to be sufficiently sensitive for the approach to be used for particle size determination. They used the form of equation (13) corresponding to a polydispersion,

$$\frac{I(\theta)}{I_0} = \int_0^\infty \left[\frac{2J_1(\alpha\theta)}{\alpha\theta}\right]^2 N(\alpha)\alpha^2 \, d\alpha. \tag{16}$$

This was transformed to yield an expression for $N(\alpha)$, the drop size distribution.

$$N(\alpha) = \frac{c}{\alpha^2}\int_0^\theta F(\alpha\theta)\phi(\theta)\theta \, d\theta, \tag{17}$$

where c is a constant, $F(\alpha\theta)$ is a tabulated function and

$$\phi(\theta) = \frac{d}{d\theta}\left[\frac{I(\theta)\pi\theta^3}{I_0}\left(\frac{2\pi}{\lambda}\right)^3\right]. \tag{18}$$

Values of $I(\theta)/I_0$ are measured and substituted into equation (17) for different values of α. In this way the distribution can be built up. Deich *et al.* used graphical methods to integrate equation (17) and claimed total errors of 15–18%. Chin *et al.* also integrated graphically and found errors up to 20%. However, good agreement can be seen between the results of this method and those from microscope counting (Fig. 11).

Cornillault [78] and Swithenbank *et al.* [79], amongst others, have approached the problem in a different way. They considered the light energy diffracted into small solid angles about 0° or at fixed angles with finite catchment angles. The former was described for a single particle by equation (15) and the latter by:

$$E_{ij} = C \cdot d^2\{[J_0^2 + J_1^2]_j - [J_0^2 + J_1^2]_i\}. \tag{19}$$

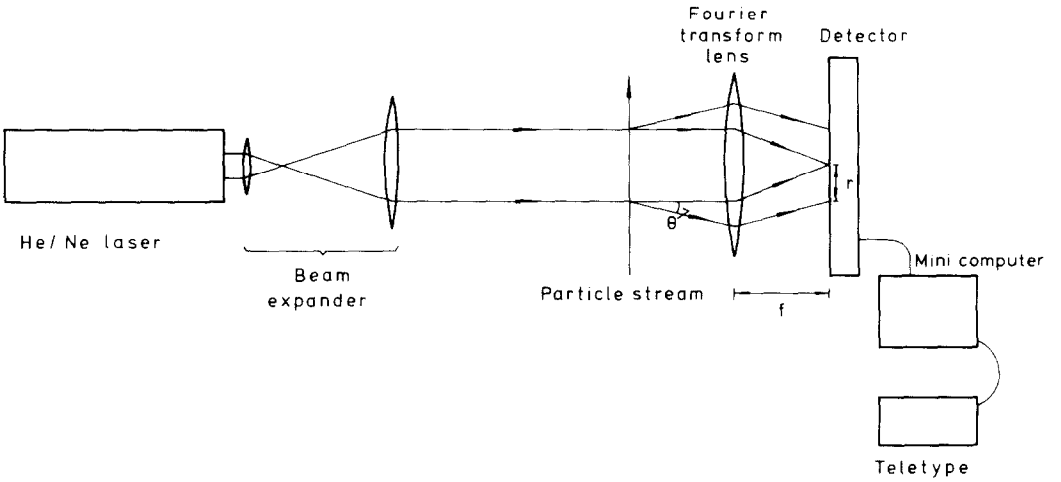

FIG. 12. Schematic of diffraction equipment and optical geometry of Fourier transform lens.

For a polydispersion this becomes:

$$E_{ij} = C' \sum_{k=1}^{\alpha} N_k(d) d_k^2 \times \{(J_0^2 + J_1^2)_{jk} - (J_0^2 + J_1^2)_{ik}\}, \quad (20)$$

which in terms of weight fractions becomes:

$$E_{ij} = C'' \sum_{k=1}^{\alpha} \frac{W_k(d)}{d_k} \times [\{J_0^2 + J_1^2\}_{jk} - \{J_0^2 + J_1^2\}_{ik}]. \quad (21)$$

If measurements are made of E_{ij} at several radii the resulting series of equations can be written as a matrix equation

$$\{E_{ij}\} = \left\{C'' \frac{W_k(d)}{d_k}\right\} \times \{(J_0^2 + J_1^2)_{jk} - (J_0^2 + J_1^2)_{ik}\}, \quad (22)$$

from which $W(d)$ can be obtained by inversion of the square matrix. However, this matrix is ill conditioned so an alternative approach is necessary. Swithenbank *et al.* assumed that the size distribution is a good approximation to a Rosin–Rammler distribution, which has the form

$$R = e^{-(d/\bar{X})^N}, \quad (23)$$

where R is the weight fraction contained in particles of diameter greater than d and $\bar{X}, N$ are characterising parameters. Initial values of the Rosin–Rammler parameters $\bar{X}, N$ are selected. The weight fraction distribution is computed through equation (23). From equation (22) the energy distribution corresponding to this Rosin–Rammler distribution is calculated and compared with the experimentally obtained energy distribution. The parameters $\bar{X}, N$ are then optimised to give the best fit. Swithenbank *et al.*, using 30 E_{ij}s, have shown the method to be sensitive to small variations in the parameters of the Rosin–Rammler distribution equation.

Two practical problems exist which are common to all the methods. The first is that light diffracted at a fixed angle from particles at different distances from the detector would arrive at different parts of the detector and cause confusion. If a lens were placed between the object and the detector so that the latter was at the focal plane of the lens then, because the lens acts as a Fourier transformer, the light diffracted by particles in a given direction is collected at one point irrespective of the position of the particle. This solution has been used by all workers. Figure 12 shows the geometry concerned. From geometric relationships and the magnification for a simple lens it can be shown that the displacement of a point from the optical axis depends only on the focal length of the lens and the angle at which the light was diffracted, i.e.,

$$r = \theta f, \quad (24)$$

where r is the displacement from the optical axis, θ is the angle of the diffracted ray, and f is the focal length of the lens.

Therefore by traversing a detector across the focal plane the light diffracted at varying angles can be detected. Because of the above relationship, equation (24), very small angles can be examined. If the maximum practicable value of r is defined then by increasing f, the minimum value of θ detectable can be made very small.

The second problem arises because the angular distribution of diffracted light varies according to the Airy function, equation (14) (Fig. 10), therefore the range of intensities to be detected fall off very rapidly and a detector with a very large range is required, larger than is practicable to achieve. Consequently alternative methods have been suggested and/or implemented to cope with this. Chin *et al.* [77] and McCreath and Beer [11] suggest the use of photographic plates and a microdensitometer. As density is a linear function of log intensity a large range of intensity can be compressed into a small range of density. Cornillault [78] has suggested the use of a mask, with apertures of varying size, for a photodetector (Fig. 13). As the detector is moved from the optical axis it is covered by a mask with an aperture

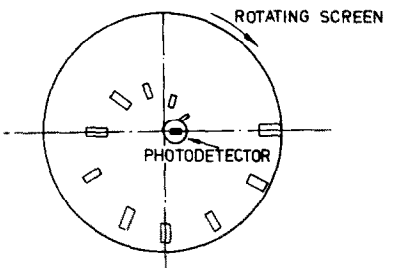

FIG. 13. Photodetector mask of Cornillault [78].

of increasing size, A. This always produces a detectable signal, $\mathscr{S}$, because

$$\mathscr{S} = \frac{E}{A} A, \tag{25}$$

and as the first right hand term decreases the second increases thus keeping the product with a manageable range. Appropriate correction must be made for the aperture size. Annular ring detectors, which would perform a function similar to the variable area mask, have been used by McSweeney and Rivers [80] and Swithenbank *et al.* [79] in conjunction with a Fourier transform lens. The area of an annular ring is proportional to the main radius if the annular thickness is constant so that the rings act in the same way as the apertures in the mask used by Cornillault. McSweeney and Rivers used a fibre bundle as the annular ring detector. One end of the bundle was grouped tightly into a circle, the other end was separated into small bundles each of which corresponded to a concentric ring at the first end. Each small ring was attached to a separate photodetector. Swithenbank *et al.* used a single chip of silicon, with annular rings on the chip sensitised as separate detectors. The width of the annular rings were not uniform but increased with increasing mean radius thus enhancing the effect shown in equation (25).

A unit using the technique of Swithenbank *et al.* is available commercially (Malvern Instruments Ltd.). This unit has been tested against suspensions of glass spheres in a specially designed stirred cell [81]. The size distributions of the suspensions were determined through an extensive photographic analysis. In most cases of unimodal distributions the Sauter mean diameters determined from the Malvern Instrument were in close agreement with those obtained from photography. Figure 14 shows an example of distributions measured using the Malvern Instrument and photography. The tests indicate that there is a concentration limit, caused by multiple scattering, of $2\ 10^9/m^3$ for a size range centred on 70 μm.

Werthemier and Wilcock [82] and Weiss and Frock [83] have produced similar methods which only produce mean particle size.

Liversey and Billmeyer [84] have reported an alternative method by which mean particle sizes may be determined from $I(\theta)$ data. They plot the data in the form of $I\theta^2$ vs θ and obtain the mean particle size from the characteristics of the resultant curve.

Shofner *et al.* [85] have produced an instrument which supplies mass flux data. They use the backscattered light and depend on the light scattered per unit volume of particle being nearly particle size independent in the range 0.3–10 μm (Fig. 15). A large probe volume is examined and the total light backscattered from all the particles in the probe volume is collected. This provides mass flux information, the instrument is limited to a range of 0.2–10 μm through Shofner *et al.* claim that the instrument could be used outside this range with appropriate calibration. However their calculations show that the backscattered light becomes increasingly particle size dependent with increasing particle size. The instrument is available commercially (Pills V, Environmental Systems Corporation).

Most other multiparticle scattering methods are not suitable for sizes in the ranges indicated in Table 1. They are, however, most useful for work on smaller particles. For further information on this

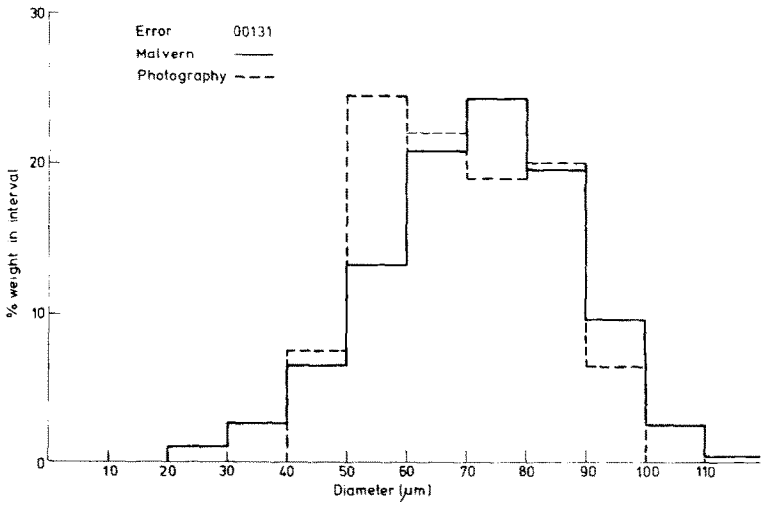

FIG. 14. Comparison of Malvern and photographic distributions—sample 1a [81].

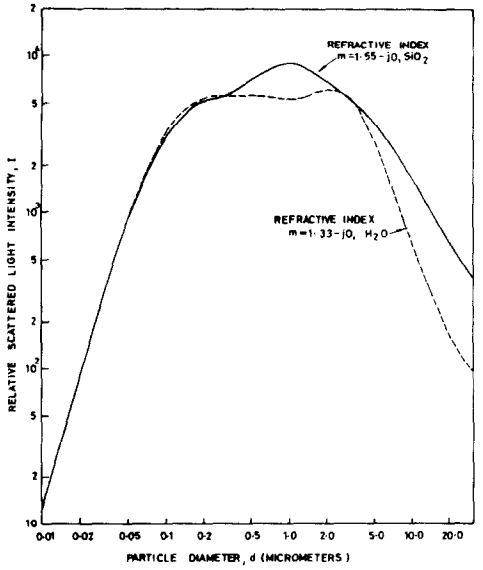

FIG. 15. Backscattered intensity per unit volume of drops – effect of drop size – after Shofner *et al.* [85].

subject the reader is referred to Williams' and Hedley's review [18].

6.1.4. *Use of holograms in scattering methods.* Holography can be used to examine the scattering from individual drops.† As noted above (Section 2.2) holograms effectively freeze a moving scene therefore reconstructed holograms may be examined at leisure. In the "freezing" the optical properties of objects are retained so that the examination could include angular scattering investigations. Tschudi *et al.* [87] have produced synthetic holograms. From computations using Mie theory the light scattering was obtained. The interference between this and unscattered lights was thence deduced and a large scale plate containing the corresponding regions of light and dark was produced and scaled down photographically. This constituted the synthetic hologram plate. They then examined the scattering by reconstructed particles at various angles.

6.2. *Obscuration, extinction and turbidity*

6.2.1. *Obscuration.* The insertion of a particle in a light beam diminishes the amount of light that emerges from the control volume along the irradiation direction. In general terms the diminution can be described as:

$$I_{out} = I_{in} - (I_{SCA} + I_{ABS}), \tag{26}$$

where I_{SCA} is the amount of light scattered in directions other than the irradiation direction and I_{ABS} is the amount of light absorbed by the particle. For single large particles the last two terms can be grouped together and the resulting group is proportional to the projected area of the particle or that part of it in the beam. If a beam of rectangular cross section is considered with the particle crossing the

†Hickling [86].

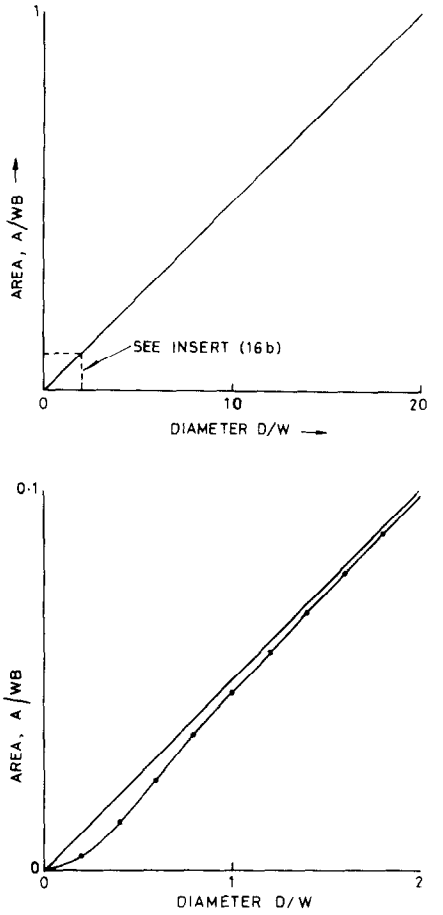

FIG. 16. (a) Obscuration area for particles crossing flat beam; (b) Insert.

longer sides then the area involved is proportional to d^2 when d is less than the beam width (shorter side). When the particle diameter is larger than the width a linear relationship is an excellent approximation. Figure 16 shows a non-dimensionalised plot of area vs diameter where the area has been non-dimensionalised with respect to the beam cross sectional area per unit breadth and the diameter with respect to the beam width. Ritter *et al.* [88] produced a flat rectangular beam by illuminating one end of a fibre bundle whose other end had been splayed out flat and used a reverse fibre bundle for observation (Fig. 17). This produced a beam 0.5 mm wide and 15 cm broad. Two of these detectors were employed, one below the other, and with them the size, velocity and frequency of streams of drops were determined. Lafrance *et al.* [89] used a similar system with a 0.25 mm wide beam. The signals from such units are electronically sorted. Coincidence errors in such systems are minimised by making the beam width as small as possible. However, as in the single particle scatter case above, should two particles pass through the beam simultaneously then the output would appear as a doublet and not a single pulse, electronic discriminators could eliminate these data points. The problems of edge effects could also be dealt with by methods similar to those of

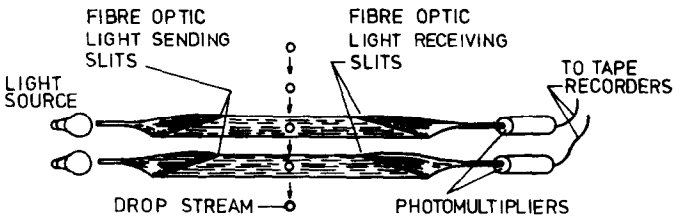

FIG. 17. Obscuration technique—schematic of equipment of Ritter *et al.* [88].

Section 6.1.2. By shining beams of another colour parallel to and just touching the working beam (on both sides) particles that are only partially in the working beam can be detected by use of beam splitters, filters and discriminators (Fig. 18).

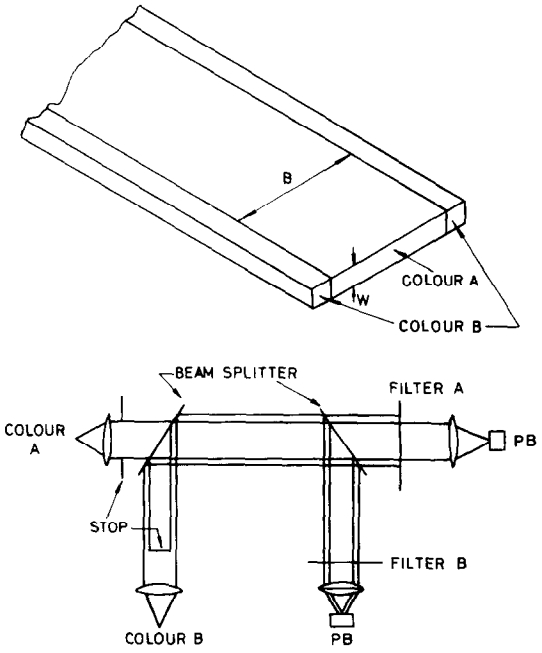

FIG. 18. Second colour masking.

A similar technique has been devised by Schleusener [90, 91] and also used by Shuster and Knollenberg [92]. A laser cavity was set up across the drop stream, in this way stronger signals, than those for ordinary obscuration, could be obtained. Schleusener claims an output sensitivity 10^4 times as great as would be due to normal photoextinction cross-sectional area subtraction. Since particles passing through the laser cavity attenuate cavity oscillations, such particles give rise to pulses in the laser output. Within a size range determined by cavity gain, cavity geometry and beam test point, the output pulse height is representative of particle size. Details of the equipment are shown in Fig. 19. The method still suffers from the problems of coincidence and edge effects however the solutions suggested above for the ordinary obscuration methods could not be applied here. Schleusener overcame the problems by directing the particles through the laser cavity by aerodynamic jetting at a suitably low concentration.

Rhodes *et al.* [93] describe an obscuration technique (Fig. 20) which eliminates the problem of absolute intensity measurement. They shone a flat laser beam through the fluid containing particles, any particle present casts a shadow. Lenses expanded the beam and shadow areas proportionally. When the beam fell onto a linear array of photodiodes the number of those covered by the shadow gave a measure of the particle size, i.e., the switched state of the photodiodes (on/off) was noted, thus eliminating the need to measure absolute light intensities.

6.2.2. *Extinction and turbidity.* The straightforward relationship between projected area and light losses do not apply for particles smaller than about 10 μm. For such particles, therefore, an alternative approach is necessary. The simultaneous presence of several particles in the probe volume would invalidate the methods described in the last

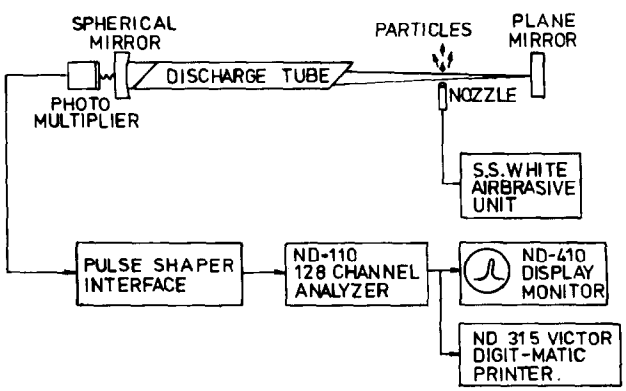

FIG. 19. Schematic for obscuration technique of Schleusener [90].

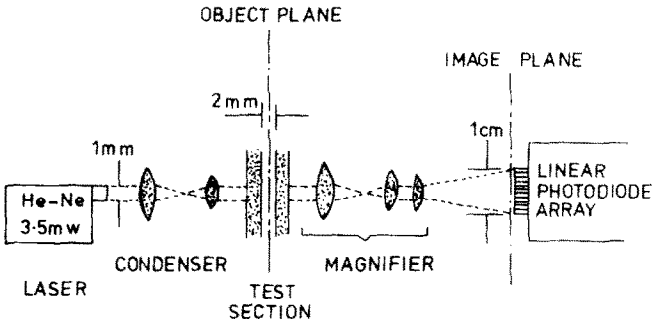

FIG. 20. Schematic for obscuration technique of Rhodes *et al.* [93].

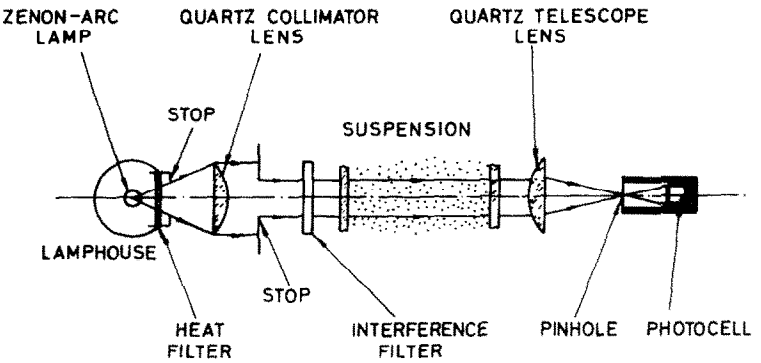

FIG. 21. Turbidity measurements – schematic of optics [95].

section. For these two cases equation (26) can be rewritten as

$$\frac{I_{out}}{I_{in}} = \exp\left(\frac{-\pi T}{4}\int_0^\infty K(\lambda, d)C_N N(d)d^2\,\mathrm{d}d\right), \quad (27)$$

where T is the optical path length in which there is particles, $K(\lambda, d)$ is defined by equation (12), and C_N is the number concentration of particles.

This may be manipulated further to give:

$$\frac{I_{out}}{I_{in}} = \exp\left(\frac{-3}{2}\frac{\bar{K}}{d_{32}}C_V T\right), \quad (28)$$

where

$$\bar{K} = \frac{\int_0^\infty K(\lambda, d)N(d)d^2\,\mathrm{d}d}{\int_0^\infty N(d)d^2\,\mathrm{d}d} \quad (29)$$

$$C_V = C_N\frac{\pi}{6}\int_0^\infty N(d)d^3\,\mathrm{d}d, \quad (30)$$

and

$$d_{32} = \frac{\int_0^\infty N(d)d^3\,\mathrm{d}d}{\int_0^\infty N(d)d^2\,\mathrm{d}d}. \quad (31)$$

For large particles ($d > 10\,\mu\mathrm{m}$) $\bar{K} = 1.0$ therefore d_{32} can be obtained from equation (27) providing the concentration is known, see, for example, Dombrowski and Wolfson [94]. For small drops $\bar{K}$ is monotonic in $\alpha_{32} = 2\pi d_{32}/\lambda$. In this case measurements are made of I_{out}/I_{in} at several wavelengths, and the log of these values plotted against the wavenumber, π/λ. The plot is then superimposed on one of $\bar{K}$ against α, and the curves moved until they coincide. The values of the Sauter mean diameter and drop concentration may then be determined. This approach was adopted by, amongst others, Walters [95] whose apparatus is shown in Fig. 21. The difference between the monodisperse and polydisperse curves of K in Fig. 9 can be used to determine the drop size distribution for $\alpha > 4$. For example, Wallach and Heller [96] prescribed the form of $N(d)$ and adjusted the constants until equation (27) was satisfied for all the wavelengths at which they took measurements.

6.3. *Laser–Doppler anemometer methods*

Laser–Doppler anemometers use the frequency information contained in light scattered by particles passing through an interference pattern (fringe pattern) to determine velocities. As the intensity of scattered light depends on particle size, the effect of size has been studied to determine its influence on the velocity measurements. The effect has also been studied by e.g., Farmer [97, 98], Fristrom *et al.* [99], Durst and Zare [100] and Hong and Jones [101] specifically to obtain particle size information. Farmer and Fristrom *et al.* independently derived a relationship between the signal visibility, the ratio of the a.c. and d.c. components of the burst of scattered light, and the ratio of particle size to fringe spacing. They both concluded that this was described by a

function of the form

$$V = \frac{2J_1(d\pi/\lambda^*)}{(d\pi/\lambda^*)}, \tag{32}$$

where J_1 is a Bessel function of the first kind, d is the particle diameter, and λ^* is the fringe spacing.

Fristrom *et al.* derived this relationship from geometric optics, confirmation being provided by Jones [102, 103] who used the more rigorous Mie theory. The calculations were carried out for a cylinder as well as a sphere, as a cylinder (say a piece of wire) can be handled more easily than a sphere and thus be very useful in proving and calibrating the method. Such a wire was used by Fristrom *et al.* in their checks of the method. The wire was repeatedly passed through the fringe system with its axis parallel to the fringes. The fringe spacing was adjusted and those spacings at which zeros occured in the Doppler burst were determined. From these a value of the diameter was calculated. This was only 5.5% different to the correct value and if a datum point whose accuracy was justifiably questioned was omitted the difference fell to 1%. Farmer checked his theoretical analysis by passing moving fringes over glass and aluminium spheres which were held onto a glass "flat" by Van der Wahl's forces. The agreement between prediction and measurement, shown in Fig. 22, can be seen to be good though it is presented on rather flattering axes.

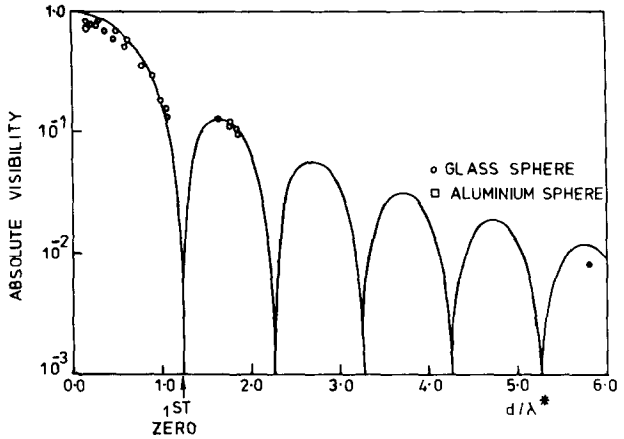

FIG. 22. Visibility of particles passing through laser fringe system—theory and experimental results of Farmer [97].

However, more rigorous calculations, Hong and Jones [101], Robards [104], Adrian and Orloff [105] and Chu and Robinson [106], have shown that the relationship shown in equation (32) only applies when the following conditions are satisfied:

(i) Light is collected in the forward scatter direction;

(ii) The Mie scattering parameter is asymptotically large ($\alpha > 60$ may be sufficient);

(iii) The collecting aperture is asymptotically large;

(iv) The laser anemometer beams are of equal power.

Workers using the more rigorous calculation approach have considered deviations from the above limitations. Robards [104] examined the effect of aperture and stop size for forward scattering. His theoretical and experimental results showed reasonable agreement. Adrian and Orloff [105] showed that for backscatter the visibility/(d/λ^*) relationship requires $\alpha = (\pi d/\lambda)$, the Mie scattering parameter as an additional parameter. They showed good agreement with the appropriate curve when examining particles of constant size at various fringe spacings (Fig. 23) and noted that the curves merged over a limited range of d/λ^*. Hong and Jones [101] determined the theoretical visibility/(d/λ^*) relationship by using full Mie theory for the scattering and determining the collected light by integrating over the collection aperture. They determined that there was a small effect of particle refractive index. By comparison of their visibility results with those from microscopic counting they showed that the error was usually about 5% and in the worst case it was still only 15%. The method has also been used on a spray by Schmidt *et al.* [107]. However, they used Farmer's simple equation relating visibility and d/λ^*, but collected the scattered light at an angle close to backscatter, i.e., well outside the range of applicability of the Farmer equation. Nevertheless, reasonable agreement was obtained between the visibility results and those from collection on a sampling slide coated with MgO, see Section 3.1. It is noted that the sample size was small; only 100 visibility signals were analysed.

The method still suffers from difficulties and disadvantages though the latter are probably far outweighed by the advantages. The first difficulty that must be overcome is that of abstracting data, the method used by Hong and Jones [101] of measuring oscilloscope traces by hand is very time consuming. For general application therefore, some automatic discriminating/measuring system is required. Such a system should not be difficult to devise. A discriminator is necessary to eliminate the need to examine each Doppler burst individually. A

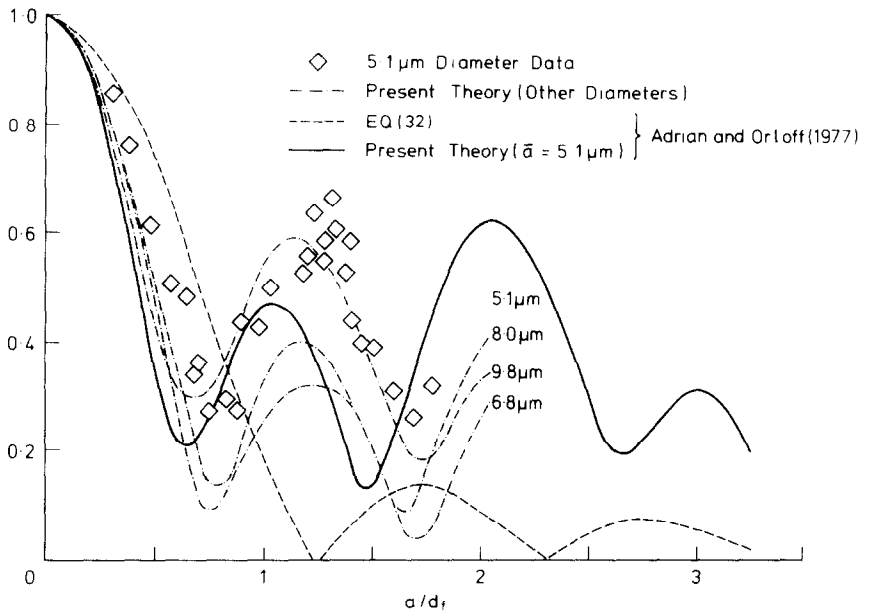

FIG. 23. Theoretical and experimental visibility for backscatter [105].

second difficulty is that the observation angle and solid collection angle must be carefully chosen to optimise the signal strength. However, Farmer has carried out a series of experiments the results of which are of great value for the above selections.

The limited range of drop sizes, discussed above, for which the visibility is an unambiguous function (fringe spacing constant) is a disadvantage of the method. If Farmer's relationship, equation (32), is applicable, then a necessary condition to avoid ambiguity is

$$\frac{d_{MAX}}{\lambda^*} < 1.22\pi, \tag{33}$$

i.e., all points fall within the first zero shown in Fig. 22. Therefore a relatively large probe volume is required as at least 10 fringes are usually required to produce a usuable signal. For geometries that do not satisfy the conditions governing equation (32) limitations similar to equation (33) exist, however they are governed by a combination of parameters determined from detailed calculations. Another disadvantage is that particles which do not pass through the centre of the probe volume yield Doppler bursts which are different from those from the centre of the probe volume (Farmer provides theoretical and experimental evidence). Thus the method will be difficult to use in the presence of "off centre" particles, however careful focussing of the cross beams and the observing optics might minimise the problem. It is this problem that makes a discriminator module in the output circuitry, necessary. The addition of a gate photomultiplier at 90° to the input light beams permits the selection of those particles passing through the centre of the probe volume, Ungut *et al.* [108]. The coincidence of two particles within the probe volume can give a spurious signal and can produce zeros when the particle/fringe spacing ratios are not equal to the normal values expected from equation (32). In these cases it is the spacing between two particles that is the controlling variable. The advantage of the method is that only one measurement detector at a fixed position is required. As the Doppler burst, which is the measured signal, also contains data on the velocity of the particle both velocity and size can be obtained particle by particle.

When equation (32) applies an alternative approach is available. This consists of using monotonically varying fringe spacing (spacing range straddling effective particle size). In this case, when the particle passes through the fringe equivalent to its size, the a.c. signal within the burst would fall to zero. This method has two disadvantages:

(i) Selection of the point of zero (or minimum) a.c. signal is difficult;

(ii) It is not easy to form a variable spacing fringe pattern. This could be achieved by passing the two beams forming the interference pattern through different parts of a prism.

Alternatively the pattern could be produced by interfering a plane wave with a circular wave.

Durst and Zare [100] have carried out experiments to assess the suitability of certain illumination/detection configurations for phase object measurement (e.g., drops, solid particles, bubbles). Most of the work related to particles outside the ranges indicated in Table 1, however one method shows possibilities for use within the indicated size range. This uses two photodetectors very close together which observe the scattered light as shown in Fig. 24a. When a particle passes through the probe volume the outputs of these photodetectors are Doppler bursts which are slightly out of phase one with the other. The phase difference is particle

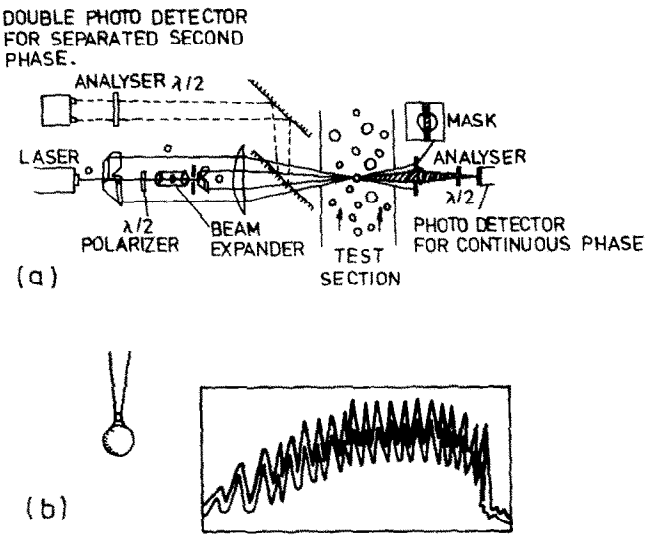

FIG. 24. Laser–Doppler approach of Durst and Zare [100]: (a) Schematic of optics and detectors; (b) Signal produced by a growing water drop.

size dependent and decreases with decreasing particle size (Fig. 24b). This makes the method less suitable for small particles but it should be possible to quantify and use this very small phase difference.

Chigier and Yule [109], Yule *et al.* [110], Ungut *et al.* [108], have also used a laser anemometry system for simultaneous drop size/velocity measurements. They, however, used the peak value of the Doppler burst to give the drop size. They determined that the signal was proportional to the square of the drop size and that the relationship could be taken as linear over limited ranges. Yule *et al.* [110] show reasonable agreement between the results of this method and those from a slide impaction technique. A disadvantage of this approach is that an absolute intensity is measured and therefore errors could arise from detector drift and fluctuation and from the effect of dirt depositing on any windows.

Another drop sizing technique using laser anemometry has been devised by Wigley [111]. However, this method is based on a time of residence approach and so will be described in Section 7 below.

Taylor [112] calculated the scattering from a small particle in a pair of crossed beams and found a modulation in the predicted envelope of the Doppler burst (Fig. 25). As can be seen the modulation appears particle size dependent. However, this modulation is not very apparent amongst the published experimental results for Doppler bursts formed by particles of the appropriate sizes.

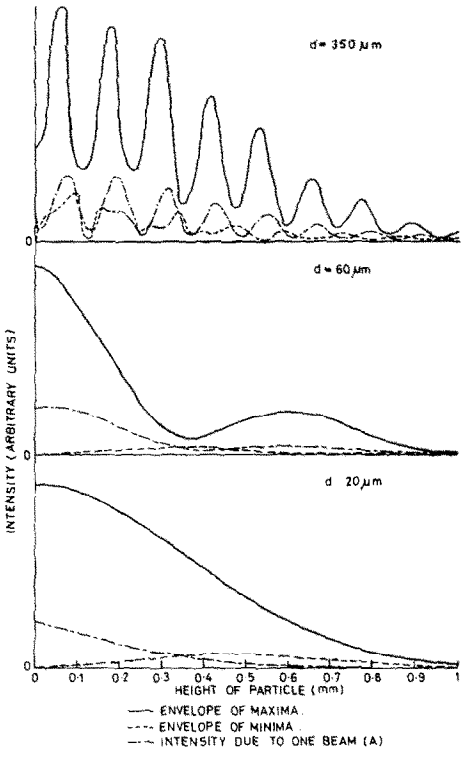

FIG. 25. Scattered interference intensities for water droplets calculated by Taylor [112].

6.4. *Sampling methods*

Very few of the instruments/techniques employing sampling of the drop laden stream followed by optical examination are suitable for the ranges of particle sizes shown in Table 1. Some instruments handle particles up to 50 μm and yet more go up to 20 μm. Most instruments were designed for aerosol sizing (usually $< 80\,\mu m$). The two problems to be considered in converting such instruments to measure drops in the range 10–1000 μm are sampling and optics. The sampling aspects are restricted by drop coalescence and deposition.† The optical aspects are governed by the concepts discussed in Section 6.1.1 however the range of configurations used prevents the formulation of any general

†See Section 3.1 for comment on this point.

guidelines. Each instrument should be examined carefully and its operational principles established. Forward scatter (Bausch and Lomb, Coulter), 90 scatter (Royco) and omnidirectional scatter (Jacobi *et al.* [113], Walsh [114]) have all been used and either one or several particles are examined at one time. In units examining particles singly coincidence errors are minimised by dilution and edge effects eliminated by directing the particles through the centre of the probe volume by aerodynamic jetting.

The instruments available have been listed by Swift [115] who includes brief descriptions of each. An independent assessment of three instruments has been presented by Whitby and Vomela [116]. Martens [117] has examined the possible errors in such units.

Multiparticle instruments use turbidity/extinction techniques and are thus most suitable for submicron particles.

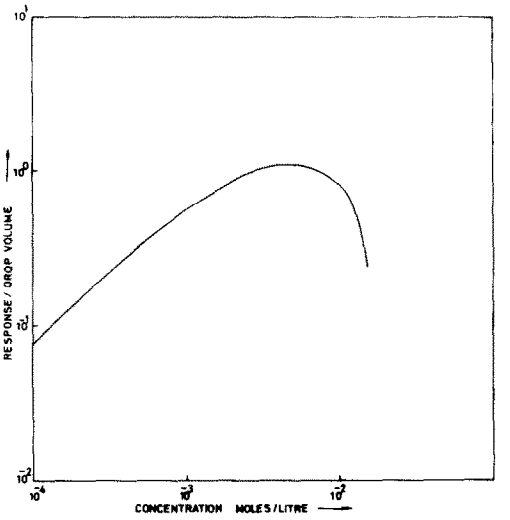

FIG. 26. Calculated response of fluorescence effect of concentration.

6.5. *Miscellaneous methods*

6.5.1. *Fluorescence.* Visible fluorescence can be excited in solutions of certain dyes by u.v. or blue light. This fluorescent light can be isolated from the u.v. by filtration. The method has been used by Benson *et al.* [118], however they only used the technique as an illumination method for photography instead of as the potentially more powerful approach of detecting the emitted intensity by photodetector. Benson *et al.* observed that drops failed to fluoresce with uniform emittance (emitted radiant flux/unit cross sectional area) both within drops and between drops. The former, they postulated, was due to a fluorescence trapping effect and the variation of the optical thickness of the drop about its cross section. The differences between drops, they claimed, were due to non-uniformity of the exciting illumination. The dependence of the fluorescence response on the dye concentration and the drop size have been determined by means of a simple analysis which allows for absorption of the exciting light, self-absorption of the fluorescence and self-quenching by the fluorescent molecules. The results of this analysis, which are qualitatively confirmed by the experimental results of Benson *et al.* [118], show that the emitted fluorescence is volume dependent. Therefore the method can be employed for mass flux monitoring. If drops are observed singly then the volume data obviously yields diameter information. This single drop approach suffers from coincidence and edge effect problems and as yet no solutions have become evident.

The concentration dependence of the fluorescence response is fairly complicated (Fig. 26). However, about the peak concentration, because of the shape of the curve, the variation is small ($\pm 30\%$ variation for a 10 fold change in concentration). Therefore the method could be used in evaporating systems.

6.5.2. *Fibre optic probes.* When light is shone down an optical fibre some is retransmitted back up the fibre because of reflection at the outer end. The amount of light reflected depends on the intensity of the original light and the refractive index of the fluid surrounding the fibre end. Consequently vapours and liquid give very different results. Based on this concept several versions of a probe have been produced as phase detectors. Such probes as designed and used by Delhaye [119] and Miller and Mitchie [120] have been employed as void fraction measuring devices. If made very small point values of void fraction are obtained.

When the probe end is not entirely covered by one phase the signal produced depends on the fraction of the cross-sectional area of the probe covered by liquid. In drop flows the probe has been used as a mass flux meter. Kennedy [121] has shown that the eccentricity of drops from the probe centre line, i.e., drops only partly on the probe, can be ignored as it does not introduce any gross errors into the mass flux measurements. Calibration measurements for drops impinging on the probe centre line are shown in Fig. 27, (the solid line is the ratio of the drop projected area to probe cross-sectional area). As can be seen use of the ratio gives an excellent approximation.

Though, as shown by Kennedy [121], drop eccentricity does not produce large errors in the mass flux measurement the same cannot be said when the probe is used to measure drop sizes. To overcome this difficulty a method of data abstraction is suggested which allows for eccentric drops. Three regions exist in the area of overlap/eccentricity relationship, they are shown in Fig. 28a–c. The relationships for the area of overlap are given below together with the limits of the eccentricity over which each applies:

$$A_0 = \frac{\pi d^2}{4} \quad 0 < e < \frac{H-d}{2} \tag{34}$$

$$A_0 = A_0(e, d) \quad \frac{H-d}{2} < e < \frac{H+d}{2} \tag{35}$$

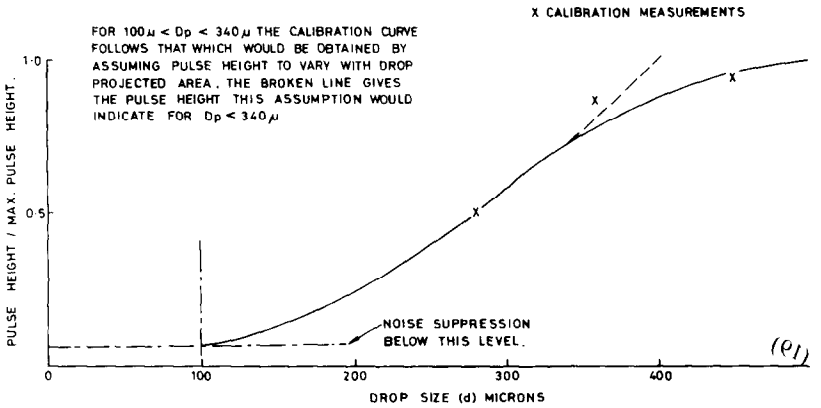

FIG. 27. Variation of light probe signal pulse height with size of water drop—probe diameter 400 μm [121].

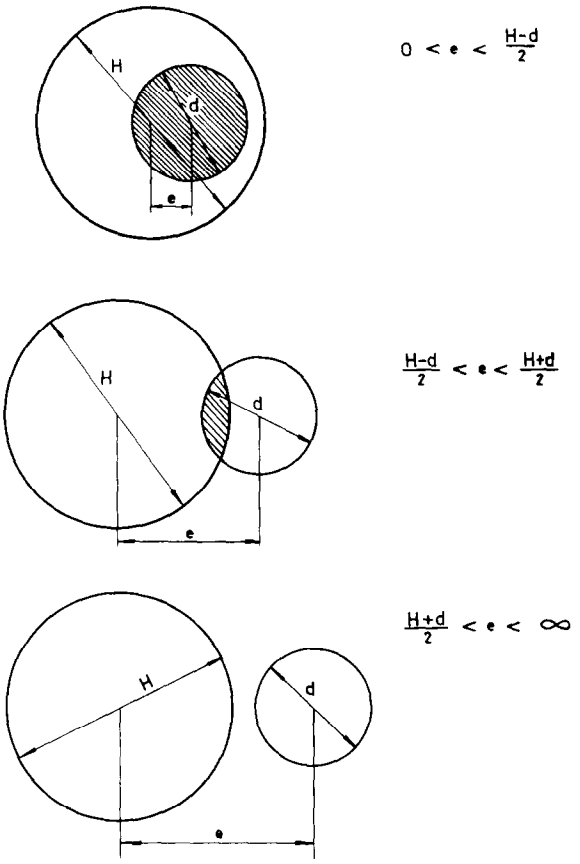

FIG. 28. Areas of overlap.

$$A_0 = 0 \quad \frac{H+d}{2} < e < \infty \tag{36}$$

where $A_0(e,d)$ is the area of overlap of two circles, an expression for which is given in Appendix I, d is the drop diameter, H is the probe cross section diameter, and e is the eccentricity.

From this it can be seen that the area of overlap is a function of two random variables, drop diameter and eccentricity. The probe measures individual areas of overlap and therefore a probability density function of area of overlap can be obtained. Popoulis [122] has shown that the probability density function of two random variables to be

$$f(A_0)dA_0 = \int_{\Delta}\int_{D_{\Delta}} f(e,d)\,de\,dd. \tag{37}$$

However e and d are not totally independent though the position of arrival of a drop centre is independent of d, the eccentricity and hence its probability depends on both the probe base size and drop size. $f(e/d)$ can be defined as the probability of an eccentricity occurring for a given drop diameter.

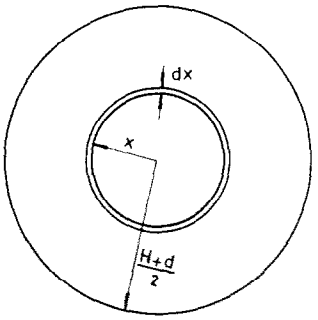

FIG. 29. Geometry for eccentricity probability calculation.

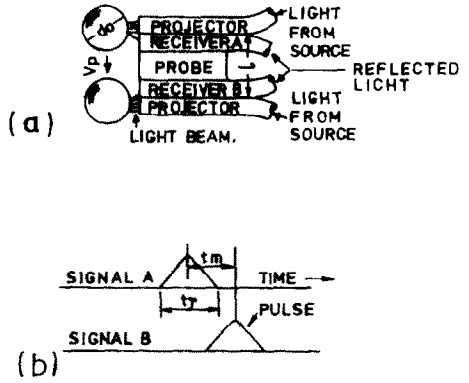

FIG. 30. Time of residence technique of Oki *et al.* [124]: (a) Schematic of fibres; (b) Representation of typical signal.

From Fig. 29 it can be seen that

$$f(e/d) = \frac{2\pi e\,de}{\pi\left(\frac{H+d}{2}\right)^2} = \frac{8e\,de}{(H+d)^2}. \quad (38)$$

Popoulis also gives

$$f(e,d) = f(e/d)f(d). \quad (39)$$

Substituting into equation (37) gives:

$$f(A_0)dA_0 = \iint_{\Delta d_1} f(e/d)f(d)\,de\,dd = \iint_{\Delta d_1} f(d)\frac{8e}{(H+d)^2}\,de\,dd. \quad (40)$$

The limits of Δd_1 are $A_{01}(e,d)$, $A_{02}(e+de, d+dd)$ which can be rearranged to give expressions for e, $e+de$, d, $d+dd$ in terms of A_{01}, A_{02} and each other. Transformation of equation (40) enables an expression for $f(d)$ to be obtained in terms of $f(A_0)$ which can be determined experimentally.

6.5.3. *Others.* Pilhofer and Miller [123] capture drops into a capillary tube and measure the length of the resultant slugs electro/optically. From these lengths the diameters of the original drops can be obtained.

7. TIME OF RESIDENCE METHODS

The techniques grouped under this heading all use the concept that the time of residence of a particle in a probe volume depends on the particle size and velocity. If the velocity and residence time are measured then the particle size can be obtained. The relationship is expressed as:

$$V = \frac{d+l}{t_R}, \quad (41)$$

where V is the particle velocity, l is a characteristic width of the probe volume, t_R is the residence time, and d is the particle diameter or chord length.

Obviously the distance l should be minimised otherwise it would overwhelm d. It should also be minimised to eliminate coincidence.

Based on this principle, Oki *et al.* [124] have used two pairs of fibre transmitters/receivers. Light is transmitted down one fibre of a pair, reflected from the particle (which is not in contact with the probe) and observed by the second fibre in the pair which is lying beside the first (Fig. 30). From the transit time between the pairs the velocity can be obtained and then from the residence time within the vision of one pair the diameter may be calculated by means of equation (41). Oki *et al.* noted that the transit time depends not only on the velocity and particle size but also on the distance between the particle and the probe, z. They assume unidirectional motion. However the residence time also depends on the eccentricity of the particle from the probe centre line, y. Use of three observation fibres surrounding a transmitter should yield sufficient transit and residence times to enable a value of the diameter to be obtained for any value of y and z. Oki *et al.* [124] used correlation techniques to obtain their mean particle size but distribution data could be obtained by calculating the size of each particle and sorting. The method also provides individual particle velocities.

Ricci *et al.* [125, 126] used an ingenious alternative method. They eliminated the need to measure the velocity of the particle being examined by using a very narrow beam of light which was scanned very rapidly in a plane perpendicular to the direction of travel of the particle. The time during which the beam was obscured was substituted into equation (41), V being taken as the scanning velocity. The error involved in using the scanning velocity instead of the more correct value, the resultant of the scanning and particle velocities, is small as long as it is considerably greater than the particle velocity (Fig. 31). To obtain the very narrow beam diameter required, Ricci *et al.* focused a laser beam, and confined the particles to the waist of the beam by use of a narrow flow cell with parallel sides. The scan does not measure a diameter but a chord of random eccentricity. However, by a method similar to that of Herringe and Davis [31], the diameter probability density function can be obtained from the measured chord probability density function.

Lading [127] used two parallel beams a short distance apart in the flow direction and observed the

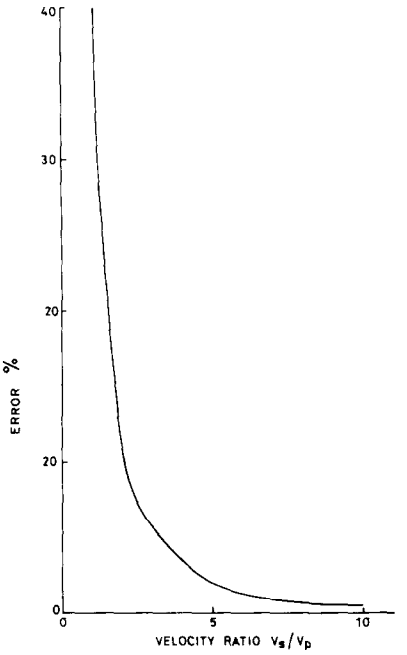

FIG. 31. Error in scanning velocity—effect of ratio of scanning to particle velocity.

obscuration of the beams. He used correlation techniques to determine velocities and gives a method of obtaining the particle size vs particle velocity spectrum. His particles were much larger than his beam so that the characteristic distance of the particle that was measured was a chord. This distance would only be a diameter when particles are constrained to pass centrally through the beam. This was done by Lading in his proving experiments.

The techniques of Ritter *et al.* [88] and Lafrance *et al.* [89] referred to in Section 6.2.1. can be adapted to give data by a time of residence method. Like Lading, the transit times between beams will yield velocities and from these and the residence times within one beam the particle sizes are obtained. With beams that are of rectangular cross section and very narrow in flow direction, as used by Ritter *et al.* [88] and Lafrance *et al.* [89], the particle will not give total obscuration but the length measured will always be a diameter. Colour edging could be provided as suggested in Section 6.2.1 to eliminate particles not totally in the beam as with these few particles a chord and not a diameter is measured.

A time of residence technique using the forward and backscatter signals from a laser anemometry system has been devised by Wigley [111]. It had previously been shown, Styles [128] that good doppler signals could be obtained from large drops. Wigley used the optical arrangement shown in Fig. 32. This gives a probe volume with a small dimension in the direction of traverse of the drops. The velocity was determined in the usual manner from the backscatter signal. In the forward direction, when a particle enters the probe volume beam 1 is reflected at the glancing angle through the slit into the photo multiplier. As the particle leaves the probe volume the same occurs with beam 2. These two events provide the photo multiplier signals which constitute the start and finish of the time of the residence. The slit aperture ensures that these signals are only produced by drops passing through the centre of the probe volume. Therefore when the velocity and residence times are substituted into equation (41) (l is considered negligible) the relevant drop dimension obtained is a diameter. From his trials Wigley determined that this method was suitable for particles in the range of 100–1000 μm. For transparent particles a third pulse is seen by the forward scatter photomultiplier, i.e. when the particle acts as a lens refracting the light of both beams into the photomultiplier slit, the central pulse is useful as it can give a measure of the sphericity of the drop.

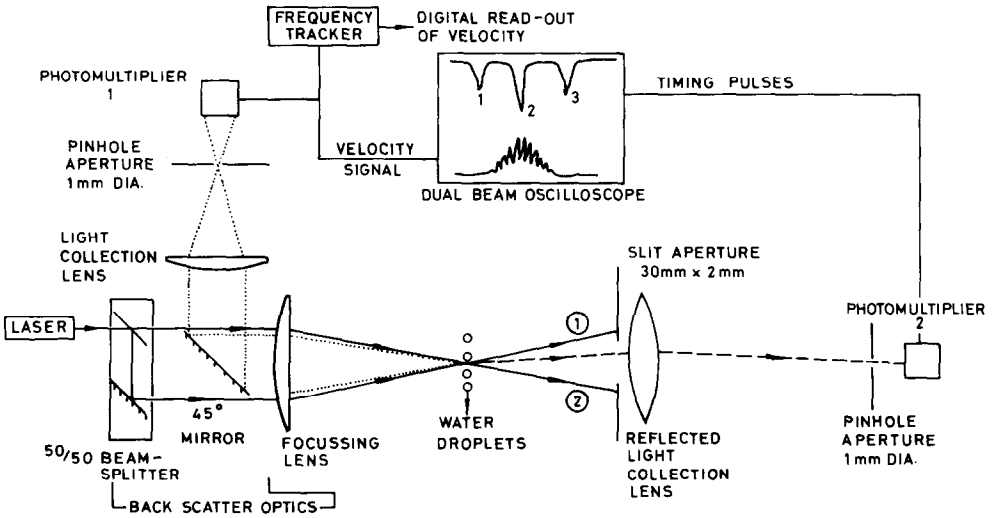

FIG. 32. Laser anemometer for droplet sizing studies, Wigley [111].

8. INDIRECT METHODS BY WAY OF VELOCITY

Workers have used velocity measurements to estimate particle size when the relationship between velocity and particle size are known. Ben Yosef *et al.* [130] have applied this method to rising bubbles and Ivanov *et al.* [131] to settling particles. Both groups used laser doppler anemometers to obtain the velocity data.

A variation on these methods has been used by Richardson and Wooding [132]. They employed an ultra microscope streak technique on settling aerosol particles. In such a technique particles normally too small to be seen can be identified as bright points of light when back illuminated. These points of light are not size dependent but velocities could be determined from the streaks formed by moving particles viewed under these conditions. Richardson and Wooding converted these velocities to particle sizes by means of the Stokes Cunningham relationship.

9. CONCLUSIONS

It is not possible to give an overall recommendation for drop size measurement methods. The optimum method depends on the type of mean or distribution required, and it is often necessary to examine the background to the requirement for drop size data. For example drop size is frequently used as an intermediate step in the calculation of some other quantity such as mass concentration or mass flux, which could be measured directly by appropriate techniques.

Photographic methods are simple but involve great tedium, with consequent possibility of error at the data abstraction stage. If automatic or semiautomatic data taking methods are used then the technique involved should be taken into account at the photographing stage so as to provide optimum input to the data reduction procedure. The "Quantimet" type of data abstraction instrument seems to allow for most of the possible errors. As data can be obtained quickly it can yield many points and so provide statistically meaningful distributions.

Amongst the other techniques it seems that the optical ones show most promise. If an overall distribution is required then the diffraction technique particularly as described by Swithenbank *et al.* [78], appears to possess admirable sensitivity to changes in both the peak value and the width of the distribution. This method is limited to the range 2–1000 μm.

For point measurements the fluorescence, laser doppler and time of residence techniques could provide the most profitable lines of approach. However none of the techniques are yet at a stage of development where they could be applied freely.

The fluorescence method, in the form suggested in the text, has no protection against coincidence and edge effect errors. As a mass flux meter the method shows great promise. In this application the effects of coincidence and edges become much less important. The Laser Doppler approach using visibility (Farmer [97], Fristrom *et al.* [99] etc.) is still limited to very small particles and work is needed to extend its range whilst preserving a small probe volume. The alternative Laser Doppler method, the phase lag approach of Durst and Zare [100], has to be proven for very small drops.

Time of residence methods are conceptually very satisfying in that they do not require a measurement of absolute light intensity. However, for such methods it is often difficult to set the threshold values at which the time intervals start and finish.

The fibre probe method described in Section 6.5.2 uses a probe inserted into the flow field. However as the experimental problems are well understood its use with the data abstraction procedure for drop sizes suggested above could well be profitable.

In cases where access to the flow field is limited the choice of method is severely restricted. Methods have to be used in spite of their shortcomings. For example, in the case where only one observation port is available the light scattering method using single particles is one of the few methods that are suitable (observation angle ~180°). This in spite of the low level of backscattered light and that the method employs measurement of absolute intensity levels.

In the cases where mass flux data is much more important than particle sizes techniques such as those described by Shofner *et al.* [84] (Section 6.1.3), Kennedy [121] (Section 6.5.2) or that employing fluorescence (Section 6.5.1) are recommended.

REFERENCES

1. J. Ahmadzadeh and J. H. Harker, Evaporation from liquid drops in free fall, *Trans. Inst. Chem. Engrs* **52**, 108 (1974).
2. R. A. Mugele and H. D. Evans, Droplet size distribution in sprays, *Ind. Engng Chem.* **43**, 1317 (1951).
3. N. Dombrowski and G. Munday, Spray drying, *Biochem. Biol. Engng Sci.* **2**, 209 (1968).
4. J. M. Delhaye, Instantaneous space averaged equation, N.A.T.O. Advanced Study Inst., Istanbul (1976).
5. J. M. Delhaye, Local instantaneous equations, N.A.T.O. Advanced Study Inst., Istanbul (1976).
6. J. M. Delhaye, Local time averaged equations, N.A.T.O. Advanced Study Inst., Istanbul (1976).
7. C. G. McCreath and J. M. Beer, A review of drop size measurement in fuel sprays, *Appl. Energy* **2**, 3 (1976).
8. L. B. Cousins and G. F. Hewitt, Liquid phase mass transfer in annular two phase flow: droplet deposition and liquid entrainment, UKAEA Report, AERE-R-5657 (1968).
9. I. G. Bowen and G. P. Davies, Particle size distribution and the estimation of Sauter mean diameter, Shell technical Note. ICT 28 (1951).
10. S. Nukiyama and Y. Tarasawa, Experiment on the atomisation of liquid by means of an air stream III distribution of the size of drops, *Trans. Soc. Mech. Engrs Japan* **4**, 86 (1938).
11. C. G. McCreath, M. F. Roett and N. A. Chigier, A technique for measurement of velocities and size of particles in flames, *J. Phys. E: Sci. Instrum.* **5**, 601 (1972).
12. C. R. Arnold and G. F. Hewitt, Further developments in the photography of two-phase gas–liquid flow, UKAEA Report AERE-R-5318 (1967).
13. K. D. Cooper, G. F. Hewitt and B. Pinchin, Photo-

graphy of two-phase flow, UKAEA Report, AERE-R-4301 (1963).
14. J. T. Pogson, J. H. Roberts and P. J. Waibler, An investigation of the liquid distribution in annular mist flow, *J. Heat Transfer* **92**, 651 (1970).
15. G. A. Kirkman and C. J. Ryley, The use of laser photography for measuring the diameters of entrained droplets in two-phase flow, Liverpool University, Dept. Mech. Engng. Report (1969).
16. C. R. Treleaven and A. H. Tobgy, Residence times micromixing and conversion in an un-premixed feed reactor—I. Residence time measurement, U. Exeter, Dept. Chem. Engng. Report No. CRE3; see also *Chem. Engng Sci.* **27**, 1653 (1972).
17. I. C. Findlay and N. Welsh, A photographic technique for determining the velocities of liquid droplets flowing in an air stream, *J. Photographic Sci.* **16**, 70 (1968).
18. I. Williams and A. B. Hedley, Size distribution measurement in aerosols. Reports on the progress of Applied Chemistry, LVII, p. 635 (1972).
19. A. Cox, *Photographic Optics*. Focal Press, London (1966).
20. N. Dombrowski and J. A. Weston, The photography of freely moving particles, *J. Photographic Sci.* **14**, 215 (1966).
21. S. C. Wakstein, The motion of small particles suspended in turbulent air flow in a vertical pipe, Ph.D. Thesis, Queen Mary College, London (1966).
22. K. V. S. Reddy, M. C. van Wijk and D. C. T. Pei, Stereophotogrammetry in particle flow investigation, *Can. J. Chem. Engng* **47**, 85 (1969).
23. P. B. Whalley, B. J. Azzopardi, L. Pshyk and G. F. Hewitt, Axial view photography of waves in annular two phase flow, UKAEA Report, AERE-R-8787 (1977).
24. S. M. de Corso, Effect of ambient and fuel pressure on spray drop size, *Trans. A.S.M.E., J. Engng Pwr* **82**, 10 (1960).
25. K. G. Birch, A spatial frequency filter to remove zero frequency, *Optica Acta* **15**, 113 (1968).
26. R. Biggs and R. L. McMillan, The errors of some haematological methods as they are used in a routine laboratory, *J. Clin. Path.* **1**, 269 (1948).
27. H. Heywood, A comparison of methods of measuring microscopial particles, *Trans. Inst. Mining Metall.* **55**, 391 (1945).
28. H. H. Watson and D. F. Mulford, A particle profile test strip for assessing the accuracy of sizing irregularly shaped particles with a microscope, *Br. J. Appl. Phys. Suppl.* No. 3, S.105 (1954).
29. B. B. Morgan and E. W. Meyer, Multichannel photoelectric scanning instrument for sizing microscopic particles, *J. Scient. Instrum.* **36**, 492 (1959).
30. C. Ramshaw, A technique for drop-size measurement by direct photography and electronic image analysis, *J. Inst. Fuel* **41**, 288 (1968).
31. R. A. Herringe and M. R. Davis, Structural development of gas–liquid mixture flow, *J. Fluid Mech.* **73**, 97 (1976).
32. A. J. Yule, N. A. Chigier and N. W. Cox, Measurement of particle sizes in sprays by the automated analysis of spark photographs, in *Particle Size Analysis* (edited by M. J. Groves). Heyden, London (1978).
33. H. C. Simmons and H. H. Gaag, US Patent 3609043 (1971).
34. M. J. Dix, H. Sawistowski and L. R. T. Tyley, Instrumentation and techniques for a direct computer-aided analysis of drop and particle systems, *Proc. 11th Int. Congress High Speed Photography* (edited by P. J. Rolls). Chapman and Hall, London (1975).
35. D. Gabor, A new microscopic principle, *Nature* **161**, 777 (1948).
36. B. J. Thompson and W. R. Zinky, Holographic detection of submicron particles, *Appl. Optics* **7**, 2426 (1968).
37. B. J. Thompson, Holographic particle sizing techniques, *J. Phys. E: Scient. Instrum.* **7**, 781 (1974).
37a. R. Bexon, Magnification in aerosol sizing by holography, *J. Phys. E: Scient. Instrum.* **6**, 245 (1973).
38. M. E. Fourney, J. H. Matkin and A. P. Waggoner, Aerosol size and velocity determination via holography, *Rev. Scient. Instrum.* **40**, 205 (1969).
39. J. M. Webster, A technique for the size and velocity analysis of high-velocity droplets and particles, *Br. J. Photography* **34**, 752 (1971).
40. T. Allen, *Particle Size Measurement*. Chapman and Hall, London (1975).
41. M. B. Ranade, D. K. Wenle and D. T. Wasan, Aerosol transport through a porous sampling probe with transpiration air flow, *J. Colloid. Interface Sci.* **56**, 42 (1976).
42. K. R. May, An ultimate cascade impactor for aerosol assessment, *J. Aerosol Sci.* **6**, 413 (1975).
43. B. Kolb, Measuring the size of droplets in wet steam, *Brown–Boveri Rev.* **49**, 350 (1962).
44. K. R. May, The measurement of airborne droplets by the magnesium oxide method, *J. Scient. Instrum.* **27**, 128 (1950).
45. R. L. Stoker, A method of determining the size of droplets dispersed in a gas, *J. Appl. Phys.* **17**, 243 (1946).
46. A. A. Putnam, F. Bennington, H. Einbinder, H. R. Hazard, J. D. Kettelle, A. Levy, C. C. Miesse, J. M. Pilcher, R. E. Thomas, A. E. Weller and B. A. Landry, Injection and combustion of liquid fuels, Wright Air Development Centre Technical Report, WADCTR 56/344, pp. 4–40 (1957).
47. S. R. M. Ellis and M. J. F. Kelly, The collection and size measurement of droplet dispersions in the presence of condensible vapours, Symposium on Interaction between Fluids and Particles, London (1962).
48. B. I. Leonchik, O. L. Danilon and E. K. Tynybekov, Rapid method of determining the dispersity of droplets in pure liquids, *Thermal Engng* **17**, 101 (1972).
49. C. A. A. van Paassen, Thermal droplet-size measurement using a thermocouple, *Int. J. Heat Mass Transfer* **17**, 1527 (1974).
50. V. W. Goldschmidt, Measurement of aerosol concentration with a hot-wire anemometer, *J. Colloid Sci.* **20**, 617 (1965).
51. J. P. Longwell, Fuel oil atomisation, D.Sc. Thesis, M.I.T. (1943).
52. E. R. Norster, Personal communication cited in McCreath and Beer (1976).
53. M. Wicks and A. E. Dukler, *In situ* measurements of drop size distribution in two-phase flow—a new method for electrically conducting liquids. In *Third Int. Heat Transfer Conf.*, Chicago, Vol. 5, p. 39 (1966).
54. S. S. McVean and G. B. Wallis, Experience with the Wicks–Dukler probe for measuring drop size distributions in sprays, Dartmouth College Report (1969).
55. J. W. Pye, Droplet size distribution in sprays using a pulse counting technique, *J. Inst. Fuel* **44**, 253 (1971).
56. A. R. Jones, Some experimental and analytical considerations of the Wicks–Dukler method for measuring droplet size distributions in sprays, C.E.G.B. Report, R/M/N866 (1976).
57. A. R. Jones and M. Sargeant, An experimental appraisal of the Wicks–Dukler technique for measuring drop sizes, C.E.G.B. Report, R/M/N930 (1977).
58. M. Beck, K. T. Lee and N. G. Stanley-Wood, A new method for evaluating the size of solid particles flowing in a turbulent fluid, *Powder Technol.* **8**, 85 (1973).
59. M. Beck, J. Drake, A. Plaskowski, N. Wainwright, Particle velocity and mass flow measurements in pneumatic conveyors, *Powder Technol.* **2**, 269.
60. J. N. Geist, J. L. York and G. G. Brown, Electronic spray analysis for electrically conducting particles, *Ind. Engng Chem.* **43**, 1371 (1951).

61. J. A. Gardener, Measurement of the drop size distribution in water sprays by an electrical method, *Instrument Practice* **18**, 353 (1964).
62. A. C. Guyton, Electronic counting and size determination of particles in aerosols, *J. Indust., Hyg. Toxical.* **28**, 133 (1946).
63. W. M. Steen and A. Chatterjee, A technique for measuring the size and number of droplets, *J. Phys. E: Scient. Instrum.* **3**, 1020 (1970).
64. D. F. Tatterson, Rates of atomisation and drop size in annular two-phase flow, Ph.D. Thesis, U. Illinois (1975).
65. G. Mie, Contributions to the optics of turbid media especially colloidal metal solutions, *Annln Physik* **25**, 377 (1908).
66. M. Kerker, *The Scattering of Light and other Electromagnetic Radiation*. Academic Press, New York (1969).
67. H. C. van de Hulst, *Light Scattering by Small Particles*. Wiley, New York (1957).
68. H. H. Blau, D. J. McCleese and D. Watson, Scattering by individual transparent spheres, *Appl. Optics* **9**, 2522 (1970).
69. I. Landa and E. S. Tebay, The measurement and instantaneous display of bubble size distribution, using scattered light, *I.E.E.E., Trans. Instrum. Measurements* **21**, 516 (1972).
70. A. Keller, The influence of cavitation nucleus spectrum on cavitation inception: Investigated with a scattered light collating method, *Trans. A.S.M.E., J. Basic Engng* **94**, 917 (1972).
71. B. J. Mason and R. Ramanadham, A photoelectric raindrop spectrometer, *Q. J. R. Meteorol. Soc.* **79**, 490 (1953).
72. F. M. Shofner, G. Kreikebaum, H. W. Schmitt and B. E. Barnhart, *In situ* continuous measurement of particulate size distributions and mass concentration using electro-optical instrumentation, Fifth Annual Industrial Air Pollution Control Conference. Knoxvill, Tennessee (1975).
73. M. D. Carabine and A. P. Moore, Light scattering instrument for kinetic measurements in aerosols with changing particle size distributions, *Faraday Symp. Chem. Soc.* **7**, 176 (1973).
74. R. A. Dobbins, L. Crocco and I. Glassman, Measurement of mean particle sizes of sprays from diffractively scattered light, *Am. Inst. Aeronaut. Astronaut. J.* **1**, 1882 (1963).
75. M. E. Deich, G. A. Saltanov and A. V. Kurshakov, Investigating the kinetics of phase transitions in shockwaves in wet steam flow, *Thermal Engng* **18**, 127 (1971).
76. M. E. Deich, G. W. Tsiklauri and V. K. Shanin, Investigation of flows of wet steam in nozzles, *High Temp.* **16**, 102 (1972).
77. J. H. Chin, C. M. Sliepcevich and M. Tribus, Determination of particle size distributions in polydisperse systems by means of measurements of angular variation of intensity of forward scattered light at very small angles, *J. Phys. Chem. Ithaca* **5**, 841 (1955).
78. J. Cornillault, Particle size analyser, *Appl. Optics* **11**, 265 (1972).
79. J. Swithenbank, J. M. Beer, D. S. Taylor, D. Abbot and G. C. McCreath, A laser diagnostic for the measurement of droplet and particle size distributions, U. Sheffield, Dept. Chem. Engng. Fuel Technol. Report also in *Exp. Diagnostics Gas Phase Combustion Systems. Prog. Astronaut. Aeronaut.* **53**, 421 (1976).
80. A. McSweeney and W. Rivers, Optical fibre array for measuring radial distribution of light intensity for particle size analysis, *Appl. Optics* **11**, 2101 (1972).
81. C. Negus and B. J. Azzopardi, The Malvern particle size distribution analyser: its accuracy and limitations, UKAEA Report, AERE-R-9075 (1978).
82. A. L. Wertheimer and W. L. Wilcock, Light scattering measurements of particle distribution, *Appl. Optics* **15**, 1616 (1976).
83. E. L. Weiss and H. N. Frock, Rapid analysis of particle size distributions by laser light scattering, *Powder Technol.* **14**, 287 (1976).
84. P. J. Liversey and R. W. Billmeyer Jr., Particle size determination by low angle light scattering: new instrumentation and a rapid method of interpreting data, *J. Colloid Interface Sci.* **30**, 447 (1969).
85. F. M. Shofner, G. Kreikebaum and H. W. Schmitt, *In situ* continuous measurement of particulate mass concentration, 68th Air Pollution Control Association Meeting, Boston (1975).
86. R. Hickling, Holography of liquid droplets, *J. Opt. Soc. Am.* **59**, 1334 (1969).
87. T. Tschudi, G. Herziger and A. Engle, Particle size analysis using computer synthesised holograms, *Appl. Optics* **13**, 245 (1974).
88. R. C. Ritter, N. R. Zinner and A. M. Sterling, Analysis of drop intervals in jets modelling obstructions of the urinary tract, *Phys. Med. Biol.* **19**, 161 (1974).
89. P. Lafrance, G. Aiello, R. C. Ritter and J. S. Trefil, Drop spectrometry of laminar and turbulent jets, *Physics Fluids* **17**, 1469 (1974).
90. S. A. Schleusener and A. A. Read, Small particle sizing using turbidimetric layered sedimentation, *Rev. Scient. Instrum.* **38**, 1152 (1967).
91. S. A. Schleusener, Automatic high-speed particle sizing using a gas laser and nuclear counter, *Powder Technol.* **1**, 364 (1968).
92. B. G. Shuster and R. Knollenberg, Detection and sizing of small particles in an open cavity gas laser, *Appl. Optics* **11**, 1515 (1972).
93. C. A. Rhodes, I. F. Stowers, L. Hawkins, R. D. Bonnell and W. Raines, In-line dynamic control monitoring of fluids for space systems, *Powder Technol.* **14**, 203 (1976).
94. N. Dombrowski and D. L. Wolfson, Measurement of the surface-volume mean diameter of sprays, *J. Aerosol Sci.* **2**, 405 (1971).
95. P. J. Walters, Optical measurements of water droplets in wet steam flows, Conference on heat and fluid flow in steam and gas turbines, p. 66 (1973).
96. M. L. Wallach and W. Heller, Experimental investigations on the light scattering of colloidal spheres, VI. Determination of size distribution curves by means of turbidity spectra, *J. Phys. Chem. Ithaca* **68**, 924 (1964).
97. W. M. Farmer, Measurement of particle size, number density and velocity using a laser interferometer, *Appl. Optics* **11**, 2603 (1972).
98. W. M. Farmer, Observation of large particles with a laser interferometer, *Appl. Optics* **13**, 610 (1974).
99. R. M. Fristrom, A. R. Jones, M. J. R. Schwar and F. J. Weinberg, Particle sizing by interference fringes and signal coherence in Doppler vilocimetry, *Faraday Symp. Chem. Soc.* **7**, 183 (1973).
100. F. Durst and M. Zare, Laser-Doppler measurements in two phase flows, U. Karlsruhe, SFB-80/TM 63 (1975).
101. N. S. Hong and A. R. Jones, A light scattering technique for particle sizing based on laser fringe anemometry, *J. Phys. D: Appl. Phys.* **9**, 1839 (1976).
102. A. R. Jones, Light scattering by a cylinder situated in an interference pattern, with relevance to fringe anemometry and particle sizing, *J. Phys. D: Appl. Phys.* **6**, 417 (1973).
103. A. R. Jones, Light scattering by a sphere situated in an interference pattern, with relevance to fringe anemometry and particle sizing, *J. Phys. D: Appl. Phys.* **7**, 1369 (1974).
104. D. W. Robards, Particle sizing user laser interferometry, *Appl. Optics* **16**, 1861 (1977).

105. R. J. Adrian and K. L. Orloff, Laser anemometer signals: visibility characteristics and application to particle sizing, *Appl. Optics* **16**, 677 (1977).
106. W. P. Chu and D. M. Robinson, Scattering from a moving spherical particle by two crossed coherent plane waves, *Appl. Optics* **16**, 619 (1977).
107. E. W. Schmidt, A. A. Boiarske, J. A. Gieseke and R. H. Barnes, Applicability of laser interferometry technique for drop size determination, Symposium on Evaporation–Combustion of fuel droplets, American Chemical Society, San Francisco (1976).
108. A. Ungut, A. J. Yule, D. A. Taylor and N. A. Chigier, Simultaneous velocity and particle size measurement in two phase flows by laser anemometry, A.I.A.A. 16th Aerospace Sciences Meeting, Huntsville, Alabama (1978).
109. N. A. Chigier and A. J. Yule, Vaporization of droplets in high temperature gas streams, Conference on Physical Chemistry and Hydrodynamics, Oxford (1977).
110. A. J. Yule, N. A. Chigier, S. Atakan and A. Ungut, Particle size and velocity measurement by laser anemometry, *J. Energy* **1**, 220 (1977).
111. G. Wigley, The sizing of large droplets by laser anemometry, UKAEA Report, AERE-R-8771 (1977).
112. A. J. Taylor, Unpublished information, AERE Harwell (1974).
113. W. Jacobi, J. Eichler and N. Stolterfoht, Particle size spectrometry of aerosols by light scattering in a laser beam, *Staub–Reinhalt–Luft* **28**, 15 (1968).
114. M. Walsh, Unpublished information, AERE, Harwell (1973).
115. D. L. Swift, Air sampling instruments 1972, American Conference of Government Industrial Hygenists, Cincinnati, Ohio (1972).
116. K. T. Whitby and R. A. Vomela, Response of single particle optical counters to non-ideal particles, *Environ. Sci. Technol.* **1**, 801 (1967).
117. A. E. Martens, Errors in measurement and counting of particles using light scattering, *J. Air Pollut. Control Assoc.* **18**, 661 (1968).
118. J. Benson, M. M. Elwakil, P. S. Myers and O. A. Uyehara, Fluorescent technique for determining the cross sectional drop size distribution of liquid sprays, *Am. Rocket Soc. J.* **30**, 447 (1960).
119. J. M. Delhaye and J. P. Galaup, Measurement of local void fraction in Freon 12 with a 0.1 mm optical fibre probe, European Two Phase Flow Meeting at AERE Harwell (1974).
120. N. Miller and R. E. Mitchie, The development of a universal probe for measurement of local voidage in liquid/gas two phase flow systems, Eleventh National A.S.M.E./A.I.Ch.E. Heat Transfer Conference, Minneapolis, p. 82 (1969).
121. T. D. A. Kennedy, Unpublished information, Harwell (1975). See also T. D. A. Kennedy and J. G. Collier, The structure of an impinging gas jet submerged in a liquid. Symposium on Multiphase flow systems, Strathclyde (1974).
122. A. Popoulis, *Probability, Random Variables and Stochastic Processes*. McGraw-Hill, New York (1965).
123. T. Pilhofer and H.-D. Miller, Photoelectric method of measuring size distribution of moderately dispersed drops in an immiscible binary liquid mixture, *Chimie-Ing. Techn.* **44**, 295 (1972).
124. K. Oki, T. Akehata and T. Shirai, A new method for evaluating the size of moving particles with a fibre optic probe, *Powder Technol.* **11**, 51 (1975).
125. R. J. Ricci, R. J. Juels, E. J. Henley and H. R. Cooper, A real time particle size analyser for filtration research and control, 64th Annual A.I.Ch.E. Meeting, New Orleans (1969).
126. R. J. Ricci and H. R. Cooper, A method for monitoring particle size distribution in process slurries, *Instrum. Soc. Am. Trans.* **9**, 28 (1970).
127. L. Lading, Analysis of a laser correlation anemometer, Third Biennial Symposium on Turbulence in Liquid, U. Missouri-Rolla, Missouri (1973).
128. A. C. Styles, Signal response of a differential Doppler laser anemometer to large scattering centres, FRCE/98/ACS/7/74 Fuel Technology and Chemical Engineering Department, Sheffield University (1974).
129. N. Ben-Yosef, O. Ginio, D. Mahlab and A. Weitz, Bubble size distribution measurement by Doppler velocimeter, *J. Appl. Phys.* **46**, 738 (1975).
130. A. P. Ivanov, A. Ya. Khurullina and A. P. Chaikovskii, Measurement of statistical parameters of scattering particles in laminar flow by Doppler spectroscopy, *Sov. Phys. Tech. Phys.* **19**, 267 (1974).
131. J. F. Richardson and E. R. Wooding, A photographic method of analysing aerosols, *J. Photographic Sci.* **4**, 75 (1956).

APPENDIX 1

CALCULATION OF THE AREA OF OVERLAP FOR ECCENTRIC DROPS

The required area is the area of overlap of two circles. However, in calculating this quantity two cases occur, these are shown in Fig. A1.1 the criterion that determines which of these occurs is the value of the X co-ordinate at the intersection of the circles. If this is larger than the eccentricity then case B is pertinent. The expressions for $A_0(e/d)$ can be derived from simple geometric considerations to be:

Case A

$$A_0 = \frac{\pi d^2}{4}\cos^{-1}\left(2\frac{(e-X_v)}{d}\right) + \frac{\pi H^2}{4}\cos^{-1}\left(\frac{2X_v}{H}\right) - e\sqrt{H^2/4 - X_v^2}$$

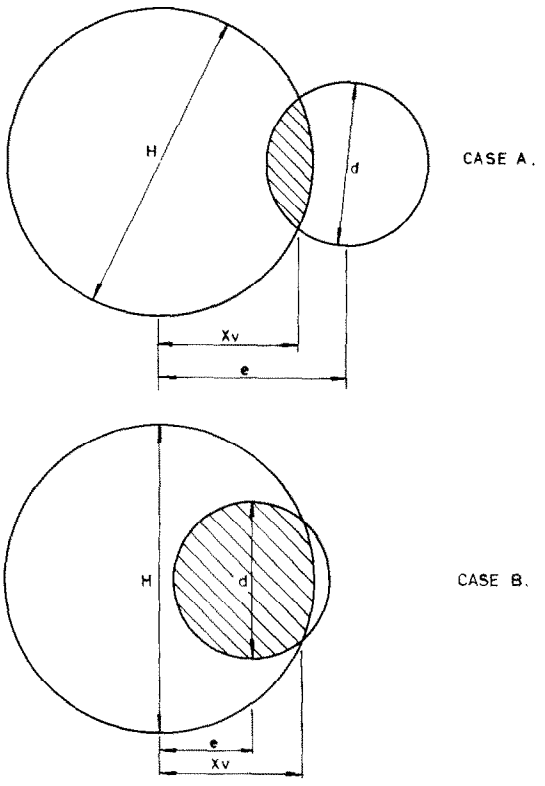

FIG. A1.1. Area of overlap.

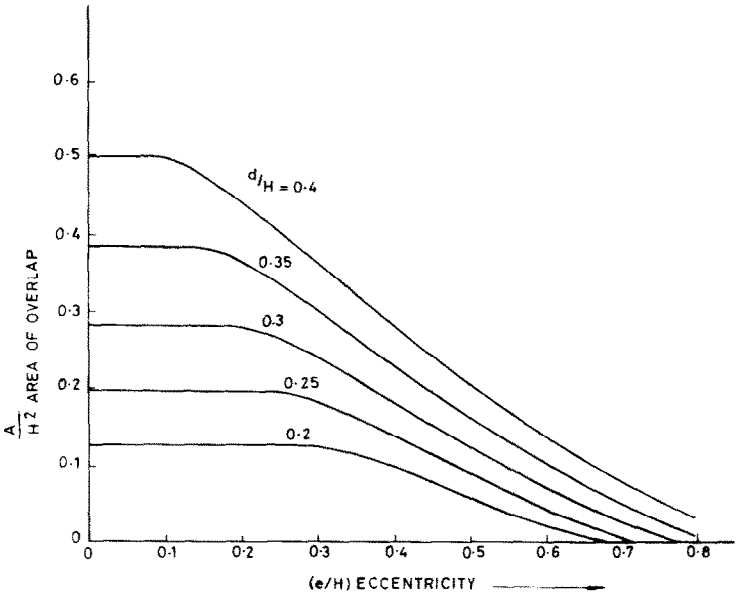

FIG. A1.2. Area of overlap—effect of eccentricity.

Case B

$$A = \frac{\pi d^2}{4} - \frac{\pi d^2}{4}\cos^{-1}\left(2\frac{(X_c - e)}{d}\right) + \frac{\pi H^2}{4}\cos^{-1}\left(\frac{2X_c}{H}\right) - e\sqrt{H^2/4 - X_c^2}.$$

Areas calculated by means of these equations are shown in Fig. A1.2. Areas are non-dimensionalised with respect to H^2 and eccentricity and drop diameter with respect to H.

APPENDIX 2

A summary table has been drawn up, this answers pertinent questions and lists important advantages and disadvantages. The summary table appears on pages 1276-1279, after the translated abstracts.

MESURE DE LA TAILLE DES GOUTTES

Résumé—On passe en revue les méthodes de mesure de la taille de gouttes, de particules solides et de bulles. On présente une sélection des méthodes potentiellement valables pour la mesure pratique de la dimension des gouttes, avec une attention particulière sur leurs difficultés et sur les sources d'erreur. On montre que la sélection d'une me)thode pour un but spécifique pose certaines questions telles que:

(1) Faut-il une moyenne ou une distribution?
(2) De quel type de moyenne ou de distribution (spatiale ou temporelle) s'agit-il?
(3) Faut-il un flux massique ou un nombre?

La méthode généralement applicable est la photographie mais elle souffre de nombreuses difficultés spécialement de la réduction des mesures. D'autres méthodes sont optiques et ne nécessitent pas l'insertion de sondes dans le fluide. Une table résume les propriétés des diverses méthodes avec référence particulière aux trois questions posées.

MESSUNG VON TROPFENGRÖSSEN

Zusammenfassung—Verfahren zur Größenmessung von Tropfen, Festkörperteilchen und Blasen wurden gesichtet. Eine Auswahl der Verfahren, die zur praktischen Messung der Tropfengröße geeignet erscheinen, wird unter besonderer Berücksichtigung ihrer Schwierigkeiten und Fehlerquellen vorgestellt. Es wird gezeigt, daß die Auswahl eines Verfahrens für den einzelnen Anwendungsfall auf bestimmte Fragen führt, nämlich: (1) Ist ein Mittelwert oder eine Verteilung gefragt? (2) Welch Form des Mittelwerts oder der Verteilung (räumlich/zeitlich) wird gesucht? (3) Wird auch nach Massenstrom oder Zahlenwerten gefragt? Das Verfahren mit dem größten Anwendungsbereich ist die Fotografie, es ist jedoch mit verschiedenen Schwierigkeiten behaftet, insbesondere hinsichtlich der Meßwertgewinnung. Die anderen geeigneten Verfahren sind optischer Art und erfordern in der Mehrzahl kein Einführen von Sonden in die Strömung. Inbegriffen ist eine tabellarische Zusammenstellung der Eigenschaften der verschiedenen Verfahren unter besonderer Beachtung der drei oben gestellten Fragen.

ИЗМЕРЕНИЕ РАЗМЕРОВ КАПЕЛЬ

Аннотация — Проведен обзор методов определения размера капель, твердых частиц и пузырьков. Методы, потенциально пригодные для практического измерения величины капель, рассмотрены с учётом их трудоёмкости и возможных погрешностей.

Показано, что в каждом конкретном случае при выборе метода необходимо ставить следующие вопросы:

(1) требуется среднее значение или распределение величин?

(2) поиск какого типа среднего значения или распределения (пространственного/временного) ведется?

(3) необходимо ли знание величины потока массы или плотности?

Чаще всего используется метод фотографирования. Однако его применение связано с рядом трудностей, особенно, при обработке и обобщении данных опытов. При использовании оптических методов, как правило, не требуется введения датчиков в поток.

Приведена таблица, где суммированы характеристики различных методов с основным упором на поставленные выше вопросы.

General Basis of Method	Detailed Basis of Method	Number of Mass Flux Data	Single Particles Counted	Distribution of Mean	Type of Distribution	Size Range μm	Disadvantages	Advantages	References (Examples)
Photography	Photography	Number and mass flux	Yes	Distribution	Spatial	5 → mm	1. Errors in data abstraction 2. Data abstraction tedious 3. Subjective judgement involved in selection of 'in-focus' drops 4. Very high quality photographs needed for automatic or semi-automatic data abstraction 5. Depth of field problems often considered	1. Very simple equipment required 2. Non disturbing to some flow fields (if unenclosed)	13 14
	Photography related methods	Number and mass flux	Yes	Distribution	Spatial/ Temporal				33 34
	Holography	Number and mass flux	Yes	Distribution	Spatial	2 → mm	1. As photography 2. Requires more equipment than photography	1. Freeze 3-D scenes which can be analysed at leisure 2. No depth of field problems	39 38
Impact	Sample slides	Number and mass flux	Yes	Distribution	Temporal	5-500	1. Disturbs flow field 2. Small drops by-pass slides	1. Counting can be effected at leisure	44
	Cascade Impactors	Number (mass flux only Cascade/Slide methods)	Yes	Distribution	Temporal	0.5-20	1. Drops deposit on sampling tube walls 2. Sampling probe head disturbs flow field		42 49

Thermal	Evaporation	Number and mass flux	Yes	Distribution	Temporal	10–300	1. Probe in flow		48
	Freezing	Mass flux	No	Distribution	Spatial/ Temporal	40–2000	1. Long freezing lengths can be necessary 2. Not suitable for liquids in contact with their own vapour		
	Freezing/Wax	Mass flux	No	Distribution	Spatial/ Temporal	10–400	1. Limited applicability because of physical properties of wax	1. Short freezing length needed	
Electrical	Resistance/Capacitance	Mass flux	No	Mean		100–2000	1. Limited to pipe flows		58
	Bridge completion	Number and mass flux	Yes	Distribution	Temporal	10–5000	1. Probe in flow 2. Data abstraction method very weak		53 54 55
	Charge removal	Number and mass flux	Yes	Distribution	Temporal	100–5000	1. Probe in flow 2. Charge density not uniform over probe 3. Controversy over signal/drop size relation		64 (Reviews other work)
Optical	Scattering by single particle at one angle	Number and mass flux	Yes	Distribution	Temporal	500–2000	1. Problems of coincidence and edge effects 2. Uses absolute intensity measurement		69
	Scattering by single particle-ratio methods	Number and mass flux	Yes	Distribution	Temporal	< 1	1. Method insensitive above 1 μm		
	Multiple particle scattering-diffraction	-	No	Distribution	Spatial/ Temporal	2–1000		1. Sensitive in changes in mean width of distribution	79
	Obscuration	Number and mass flux	Yes	Distribution	Spatial/ Temporal	50–1000	1. Uses absolute intensity measurements 2. Not space specific	1. Signal/diameter relation linear for large particles	88
	Obscuration - detector counting	Number and mass flux	Yes	Distribution	Spatial/ Temporal	10–100	1. Not space specific	1. Does not use absolute intensity measurements	93
	Turbidity	-	No	Mean	-		1. Most suitable for very small particles	1. Only measures d_{32}	74 95

General Mass of Method	Detailed Basis of Method	Number of Mass Flux Data	Single Particles Counted	Distribution of Mean	Type of Distribution	Size Range μm	Disadvantages	Advantages	References (Examples)
Optical - continued	Laser doppler - Visibility	Number and mass flux	Yes	Distribution	Temporal	< 10	1. Ambiguity if fringe spacing $\leq Kd_{max}$ 2. Simple relationships only exist for limited conditions, e.g. forward scatter 3. Analysis and relationships very complex in backscatter	1. Also provides velocity	97,98,99, 101,104, 105,107
	Laser doppler - Variable fringe spacing	Number and mass flux	Yes	Distribution	Temporal	Not known	1. Variable fringe spacing difficult to produce 2. Point of equivalent size difficult to determine		99
	Laser doppler - Phase lag	Number and mass flux	Yes	Distribution	Temporal	Not known	1. Very small phase differences to be measured	1. Also provides velocity	110
	Laser doppler - Envelope modulation	Number and mass flux	Yes	Distribution	Temporal	Not known	1. Expected modulations not seen in experiments		112
	Sampling followed by optical analysis	Number and mass flux	Yes	Distribution		1-80	1. Sampling disturbs flow structure 2. Larger drops will deposit on sample tube walls		113,115
	Fluorescence	Number and mass flux	Yes	Distribution	Temporal	Not known	1. Coincidence and edge effects (no solution known) 2. Uses absolute intensity measurements 3. Concentration sensitive	1. Can provide mass flux data	

Optical - continued	Fluorescence - photography	Number and mass flux	Yes	Distribution	Spatial	1 → mm	1. Special camera required 2. Non-uniform fluorescence might occur		118
	Fibres	Number and mass flux	Yes	Distribution	Temporal	100–400	1. Probe in flow stream 2. Slow removal of drops in dense sprays 3. Data abstraction method incomplete 4. Lower limit set by noise		121
Time of Residence	Fibres	Number and mass flux	Yes	Distribution	Temporal	200–1000	1. Probe in flow 2. Distance of drops from probe and from probe centre line important but not allowed for (can be overcome)	1. Also provides velocities	124
	Laser anemometer	Number and mass flux	Yes	Distribution	Temporal	100–1000	1. Needs good access	1. Also provides velocities 2. Can identify non-spherical particles	111
	Scanning beam	Number and mass flux	Yes	Distribution	Temporal	10–1000	1. Limited to flow through narrow cell 2. Measures chord length 3. Not space specific (though could be made so)		126
	Beam Interrupt	Number and mass flux	Yes	Distribution	Spatial/ Temporal		1. Not space specific 2. Coincidence and edge effects 3. Can measure chord		127
	Needle Contact	Number and mass flux	Yes	Distribution	Temporal		1. Most suitable for bubbles 2. Problems due to drop deformation/breakup on first needle	1. Also provides velocities	31
Indirect via Velocity		Number and mass flux	Yes	Distribution	Temporal		1. Limited to situations where exact V/d relation known		130,131